Investigating Mechanisms of Acquired Resistance to CHK1 Inhibitors in the Human Ovarian Cancer Cell Line PEO1

Natasha Anne Tappenden

MSc by Research (Cell Biology)

School of Biosciences

University of Kent

Supervisor:

Professor Michelle Garrett

Declaration

No part of this thesis has been submitted in support of an application for any degree or qualification of the University of Kent or any other university or institute of learning.

Natasha Anne Tappenden

Acknowledgements

I would like to thank my supervisor Professor Michelle Garrett for her continued support and guidance throughout the entirety of the project.

I would also like to thank everyone in the Garrett lab including, Edith Blackburn, Nathan Breeds, Jasmine Jakubowski, Helen Grimsley, Daniel Cherry and Nova Dora.

In addition, I would also like to thank my family and friends for their continued love and support throughout this year and the three previous years while studying at the University of Kent.

Finally, I would like to thank the Kent Cancer Trust for their contribution towards funding the project.

Table of Contents

Abbreviations

ABC	Adenosine triphosphate-binding cassette transporter
ATM	Ataxia telangiectasia mutated
ATR	*Ataxia telangiectasia* and Rad3-related protein
ATRIP	ATR interacting protein
BSO	Bilateral salpingo-oophorectomy
CDK	Cyclin-dependent kinases
CREB	cAMP response element binding protein
DDR	DNA damage response
DNA-PK	DNA-dependent protein kinase
DSB	Double-stranded break
EGFR	Epidermal growth factor receptor
FBS	Foetal bovine serum
FHA	Forkhead-associated domain
FIGO	International federation of gynaecology and obstetrics
HRR	Homologous recombination repair
IMDM	Iscoves modified dulbecco's medium
KD	Kinase domain
MDR	Multi-drug resistance
PARP	Poly-(adenosine diphosphate-ribose)
PBS	Phosphate-buffered saline
PIKK	Phosphatidylinositol-3-kinase-related kinase
RPA	Replication protein A
RPMI	Rosewell park memorial institute
SCD	SQ/TQ cluster domain
SCF	Skp1-Cul1-F box
SRB	Sulforhodamine B
SSB	Single-stranded DNA break
ssDNA	Single-stranded DNA
TCA	Trichloroacetic acid

List of Figures

List of Tables

Abstract

The CCNE1 gene, which encodes the protein Cyclin E, is amplified in 20% of high-grade ovarian carcinomas. The amplification of CCNE1 is associated with the development of chemotherapeutic resistance. The overexpression of Cyclin E is also associated with high levels of replication stress. Ovarian cancer cells with CCNE1 amplification have been found to be more proficient at homologous-recombination repair, which might be necessary for the survival of cells overexpressing Cyclin E. The checkpoint kinase CHK1 is a key regulator of DNA repair by homologous recombination. Therefore, CHK1 inhibition may induce synthetic lethality in cells overexpressing Cyclin E. The CHK1 inhibitors SRA737 and Prexasertib are currently being clinically evaluated in ovarian cancer patients. It is useful to understand potential mechanisms of resistance even when a drug is in clinical development, to help optimise how it will be used. The aim of the project was to generate and characterise resistance to CHK1 inhibitors, SRA737 and Prexasertib, in PEO1 ovarian cell line models. The resistant cell lines were generated using a dose escalation strategy and characterised using western blotting and drug profiling techniques. The SRA737- and Prexasertib-resistant cell lines were not only resistant to their respective CHK1 inhibitor, but were cross-resistant to Prexasertib and SRA737, respectively. The resistant cell lines were also cross-resistant to the ATR inhibitor AZD6738 but displayed sensitivity to the ATM inhibitor AZD0156. Western blot analysis of basal DDR proteins revealed some changes in DDR signalling between the parental versus the resistant cell lines. However, the most significant findings came from the dose-response western blots, in which we saw strong induction of γH2AX in the parental cell line in response to increasing concentrations of Prexasertib, but very limited induction in the Prexasertib-resistant cell line, which may suggest that DNA repair plays a critical role in the development of Prexasertib resistance.

1.0 Introduction

1.1 An Overview of Ovarian Cancer

In 2015, it was estimated that there are around 7,400 new cases of ovarian cancer each year in the UK. Ovarian cancer is the 6th most common cancer for females in the UK. In 2016, is was estimated that there are around 4,100 deaths related to ovarian cancer in the UK each year, and it was estimated that only a third (35%) of woman diagnosed with ovarian cancer in England and Wales survive their disease for 10 years or more. Since the early 1990's, the incident rates for ovarian cancer in the UK have remained relatively constant. Only over the past 10 years have the incident rates for ovarian cancer in the UK decreased by 5% (*Ovarian cancer statistics | Cancer Research UK*).

1.2 Histological Subtypes of Ovarian Cancer

Typically, ovarian cancer (benign or malignant) arises from one of three cell types including; epithelial cells, stromal cells and germ cells, however ovarian cancer is a heterozygous disease and has multiple histological subtypes. For example, epithelial cell tumours are comprised of 5 main histotypes including high-grade serous, endometrioid, clear cell, mucinous and low grade serous (Brett M. *et al.*, 2017). Most ovarian tumours, approximately 85-95%, originate from epithelial cells and typically occur in women older than 50 years. Stromal cell tumours account for approximately 5-8% of all ovarian carcinomas, and may occur in woman of any age, however certain histological subtypes such as Sertoli-Leydig (androblastomas) are more likely to occur during adolescence. Germ cell tumours are more likely to occur in children and young adults between the ages of 20-30 years, and account for approximately 3-5% of all ovarian carcinomas (Roett and Evans, 2009).

1.3 Staging and Grading of Ovarian Cancer

The stage of ovarian cancer refers to the extent to which the disease has spread and is classified according to International Federation of Gynaecology and Obstetrics (FIGO) guidelines (Figure 1.1.) The FIGO system classifies ovarian cancer into four stages; where a low number, such as stage I, refers to a cancer that has remained localised to the primary tumour, and a high number, such as stage IV, refers to a cancer that has metastasised and spread to other parts of the body (Han and Coleman, 2007).

Stage I. Tumor confined to ovaries or fallopian tube(s)
T1-N0-M0
IA: tumor limited to one ovary (capsule intact) or fallopian tube; no tumor on ovarian or fallopian tube surface; no malignant cells in the ascites or peritoneal washings
T1a-N0-M0
IB: tumor limited to both ovaries (capsules intact) or fallopian tubes; no tumor on ovarian or fallopian tube surface; no malignant cells in the ascites or peritoneal washings
T1b-N0-M0
IC: tumor limited to one or both ovaries or fallopian tubes, with any of the following:
IC1: surgical spill
T1c1-N0-M0
IC2: capsule ruptured before surgery or tumor on ovarian or fallopian tube surface
T1c2-N0-M0
IC3: malignant cells in the ascites or peritoneal washings
T1c3-N0-M0

Stage II. Tumor involves one or both ovaries or fallopian tubes with pelvic extension (below pelvic brim) or primary peritoneal cancer
T2-N0-M0
IIA: extension and/or implants on uterus and/or fallopian tubes and/or ovaries
T2a-N0-M0
IIB: extension to other pelvic intraperitoneal tissues
T2b-N0-M0

Stage III. Tumor involves one or both ovaries or fallopian tubes, or primary peritoneal cancer, with cytologically or histologically confirmed spread to the peritoneum outside the pelvis and/or metastasis to the retroperitoneal lymph nodes
T1/T2-N1-M0
IIIA1: positive retroperitoneal lymph nodes only (cytologically or histologically proven):
IIIA1(i) Metastasis up to 10 mm in greatest dimension
IIIA1(ii) Metastasis more than 10 mm in greatest dimension
IIIA2: microscopic extrapelvic (above the pelvic brim) peritoneal involvement with or without positive retroperitoneal lymph nodes
T3a2-N0/N1-M0
IIIB: macroscopic peritoneal metastasis beyond the pelvis up to 2 cm in greatest dimension, with or without metastasis to the retroperitoneal lymph nodes
T3b-N0/N1-M0
IIIC: macroscopic peritoneal metastasis beyond the pelvis more than 2 cm in greatest dimension, with or without metastasis to the retroperitoneal lymph nodes (includes extension of tumor to capsule of liver and spleen without parenchymal involvement of either organ)
T3c-N0/N1-M0

Stage IV. Distant metastasis excluding peritoneal metastases
Stage IVA: pleural effusion with positive cytology
Stage IVB: parenchymal metastases and metastases to extra-abdominal organs (including inguinal lymph nodes and lymph nodes outside of the abdominal cavity)
Any T, any N, M1

Figure 1.1. FIGO Ovarian Cancer Staging System. (Prat and FIGO Committee on Gynecologic Oncology, 2015)

Epithelial cell tumours are further subclassified by histological grading. The grading of non-serous carcinomas is based on architectural or cytological features such as nuclear atypia. The system assigns non-serous carcinomas a grade between 1-3, where grade 1 refers to a well differentiated cancer which strongly resembles that of a normal cell, and grade 3 refers to a poorly differentiated cancer that appears abnormal in comparison to normal cells. This grading system does not apply to serous carcinomas, which are graded using a two-tier grading system. Serous carcinomas are subclassified into either high- or low-grade depending on the status of the *TP53* gene. Typically, high-grade serous carcinomas harbour *TP53* mutations, whereas low-grade serous carcinomas contain wild-type *TP53* but harbour *K-RAS* and *B-RAF* mutations (Berek, Crum and Friedlander, 2015).

1.4 Treatment of Ovarian Cancer

The treatment for ovarian cancer is dependent on several factors including the histological subtype, as well as the stage and grade of the disease. The main treatments for ovarian cancer are surgery and chemotherapy, however for those patients with advanced ovarian cancer there are additional treatment options including targeted therapy, hormone therapy and radiotherapy (PDQ Adult Treatment Editorial Board, 2002).

1.4.1 Surgery for Ovarian Cancer

In patients with early stage ovarian cancer, surgery is primarily used for accurate staging which involves total abdominal hysterectomy and bilateral salpingo-oophorectomy (BSO), followed by omentectomy. Staging biopsies can also be obtained from the pelvic and para-aortic lymph nodes via retroperitoneal lymph node dissection. If the patient presents with mucinous ovarian cancer, then an appendectomy should also be performed as the appendices are involved in mucinous ovarian cancer (Han and Coleman, 2007).

In patients with advanced ovarian cancer, surgery is primarily used for disease debulking which involves removing the primary tumour and is commonly referred to as optimal cytoreduction. The definition of optimal cytoreduction remains controversial, however it is largely defined as residual tumours less than 1cm. It has been demonstrated that optimal cytoreduction of tumour burden is associated with significantly improved patient survival outcomes (Han and Coleman, 2007).

1.4.2 Chemotherapy for Ovarian Cancer

Chemotherapy can be used alone or in combination with other types of treatment for ovarian cancer. For example, patients may start chemotherapy before (neoadjuvant chemotherapy) or after surgery (adjuvant chemotherapy). The most common chemotherapeutic drug used in the treatment of ovarian cancer is Carboplatin, and it is often used in combination with another chemotherapeutic drug known as Paclitaxel (CarboTaxol) (Boyd and Muggia, 2018). CarboTaxol is administered intravenously and is usually given once every three weeks, where each three-week period is a cycle of treatment and each patient typically receive 3-6 cycles. (Masoumi-Moghaddam *et al.*, 2015).

Carboplatin is a derivative of Cisplatin; it has a similar mechanism of action but differs in terms of its structure and toxicity. Cisplatin and Carboplatin are platinum-based compounds that each possess two ammonia groups and one leaving group. The leaving group for Cisplatin consists of two chloride atoms, whereas the leaving group for Carboplatin is a cyclobutane moiety (Figure 1.2.) (Go and Adjei, 1999). It is the leaving groups that results in the differences in each platinum drugs toxicity. Platinum drugs undergo aquation which results in the formation of positively charged molecules that can interact with the DNA to form platinum/DNA adducts (McWhinney, Goldberg and McLeod, 2009).

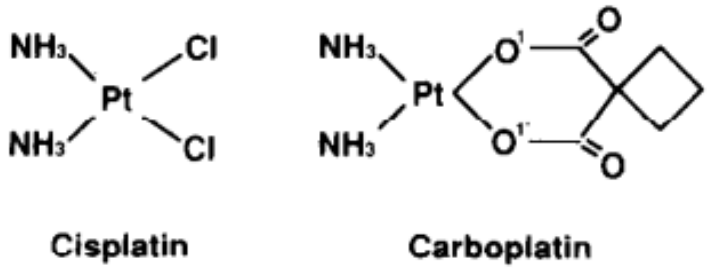

Figure 1.2. The Chemical Structure of Cisplatin and Carboplatin. (Hongo *et al.*, 1994)

Paclitaxel is a microtubule stabilising agent. Microtubules are long, filamentous structures made up of alternating α- and β-tubulin subunits. Microtubules form part of the cytoskeleton and are essential in several cellular processes including, cell shape, intracellular transport, cell signalling, cell division and mitosis. Paclitaxel binds to the β- tubulin subunit, thereby stabilising the microtubule and increasing microtubule polymerisation, which in turn leads to cell death (Alqahtani *et al.*, 2019).

1.5 Molecular Targeted Therapy for Ovarian Cancer

Despite recent advances in surgical techniques and the use of chemotherapeutic agents, relapse or recurrence continues to be a major problem in the treatment of ovarian cancer. The unmet need of relapse- or recurrent ovarian cancer patients, along with an improved understanding of ovarian cancer biology has led to the development of molecular targeted therapies. Molecular targeted therapy is a type of cancer treatment that uses small-molecule inhibitors or monoclonal antibodies to target biological pathways crucial for cancer cell survival. (Yap, Carden and Kaye, 2009).

1.5.1 Olaparib (Lynparza)

Olaparib is a poly-(adenosine diphosphate-ribose) polymerase (PARP) inhibitor. PARP plays an essential role in the base excision repair of single-stranded DNA breaks (SSBs). PARP inhibition results in the accumulation of SSBs, which can lead to the formation of double-stranded DNA breaks (DSBs) following replication fork stalling or collapse (Hutchinson, 2010). DSBs cannot be repaired in tumours with defects in homologous recombination repair (HRR), owing to mutations in BRCA1 or BRCA2. About 15% of women with ovarian cancer carry a mutation in BRCA1 or BRCA2. PARP inhibition induces synthetic lethality in BRCA-deficient ovarian cancers (Ledermann *et al.*, 2012). Olaparib is the first targeted treatment to exploit DNA damage response (DDR) deficiencies, such as BRCA mutations, to preferentially kill cancer cells.

1.6 DNA Damage Response

To ensure faithful replication and genome stability, cells have evolved to initiate cell cycle arrest, DNA repair and apoptosis, this is collectively known as the DNA damage response (DDR) (Huen and Chen, 2008) (Figure 1.3.). The DDR is primarily mediated by the ataxia telangiectasia-mutated (ATM) and ataxia telangiectasia and Rad3-related (ATR) protein kinases. ATM and ATR are members of the phosphatidylinositol-3-kinase-related kinase (PIKK) family of proteins, and recognise proteins with the consensus sequence [ST]-Q. The best characterised ATM/ATR substrates are the checkpoints kinases CHK1 and CHK2 (Awasthi, Foiani and Kumar, 2015).

1.6.1 Structure and Activation of CHK1/CHK2

CHK1 consists of an N-terminal kinase domain and a C-terminal regulatory domain (Walker *et al.*, 2009). ATR phosphorylates CHK1 on residues S317 and S345 which triggers CHK1 activation. In the absence of DNA damage CHK1 appears to adopt a close conformation which blocks the CHK1 kinase domain. It has been suggested that the ATR-dependent phosphorylation of CHK1 may disrupt the closed conformation so that the kinase domain is exposed to downstream substrates (Han *et al.*, 2016).

In contrast, CHK2 consists of an N-terminal SQ/TQ cluster domain (SCD), a central forkhead-associated (FHA) domain, and a C-terminal kinase domain (KD). ATM phosphorylates CHK2 on several residues including T68 located within the N-terminal SCD domain. The SCD domain phosphorylation triggers CHK2 dimerization, in part through intermolecular phospho-T68-FHA domain interactions. Dimerization promotes kinase activation through activation-loop autophosphorylation on residues T383 and T387, along with residue S516 located within the CHK2 C-terminal domain (Cai, Chehab and Pavletich, 2009).

1.6.2 CHK1/CHK2 Signalling Outputs

The best characterised CHK1/CHK2 substrates are CDC25 dual-specificity phosphatase family members, CDC25A and CDC25C. The CDC25 phosphatases control cell cycle progression by regulating CDK activity through dephosphorylation of inhibitory residues T14 and Y15 (Hughes *et al.*, 2013). CHK1 and CHK2 phosphorylate CDC25C on residue S216, which creates a binding site for members of the 14-3-3 family of proteins (Peng *et al.*, 1997). It has been suggested that the binding of 14-3-3 proteins promotes the cytoplasmic retention/nuclear exclusion of CDC25C, which as a result prevents CDC25C from activating CDK1-Cyclin B thereby delaying entry into mitosis (Dalal *et al.*, 1999). In addition, CHK2 phosphorylates CDC25A on residue S123, which in turn targets CDC25A for ubiquitin-mediated proteasomal degradation (Falck *et al.*, 2001). CHK1 has also been found to phosphorylate residue S123 of CDC25A, along with residues S178, S278 and S292, however this activity is dependent on the ATM-mediated activation of CHK1. As a result, CDC25A can no longer activate CDK2-Cyclin E/A thereby delaying S-phase entry and progression, respectively (Sørensen *et al.*, 2003). Taken together, the phosphorylation of CDC25 phosphatases explains in part how CHK1 and CHK2 regulate cell cycle arrest in response to DNA damage.

In response to DNA damage, the p53 protein is activated which in turn regulates a number of cellular processes including, cell cycle arrest, DNA repair, senescence and apoptosis (Harris and Levine, 2005). The protein p53 has a short half-life in normal cells, in part due to its rapid degradation mediated by MDM2. The protein MDM2 is an E3-ubiqutin ligase that targets p53 for proteasome-mediated degradation (Moll and Petrenko, 2003). CHK1 and CHK2 phosphorylate p53 on residue S20 which abrogates the binding of MDM2 and increases the stability of p53 (Shieh *et al.*, 2000). In addition, ATM phosphorylates residue S395 of MDM2, which attenuates the ability of MDM2 to promote the nuclear export and degradation of p53 (Maya *et al.*, 2001). ATM, along with ATR and DNA-PK, also phosphorylates p53 on residue S15 which promotes the transactivation activity of p53 (Dumaz and Meek, 1999). Therefore, CHK1 and CHK2, as well as several other DDR proteins, stabilise and activate p53 through phosphorylation of p53 itself and its negative regulator MDM2.

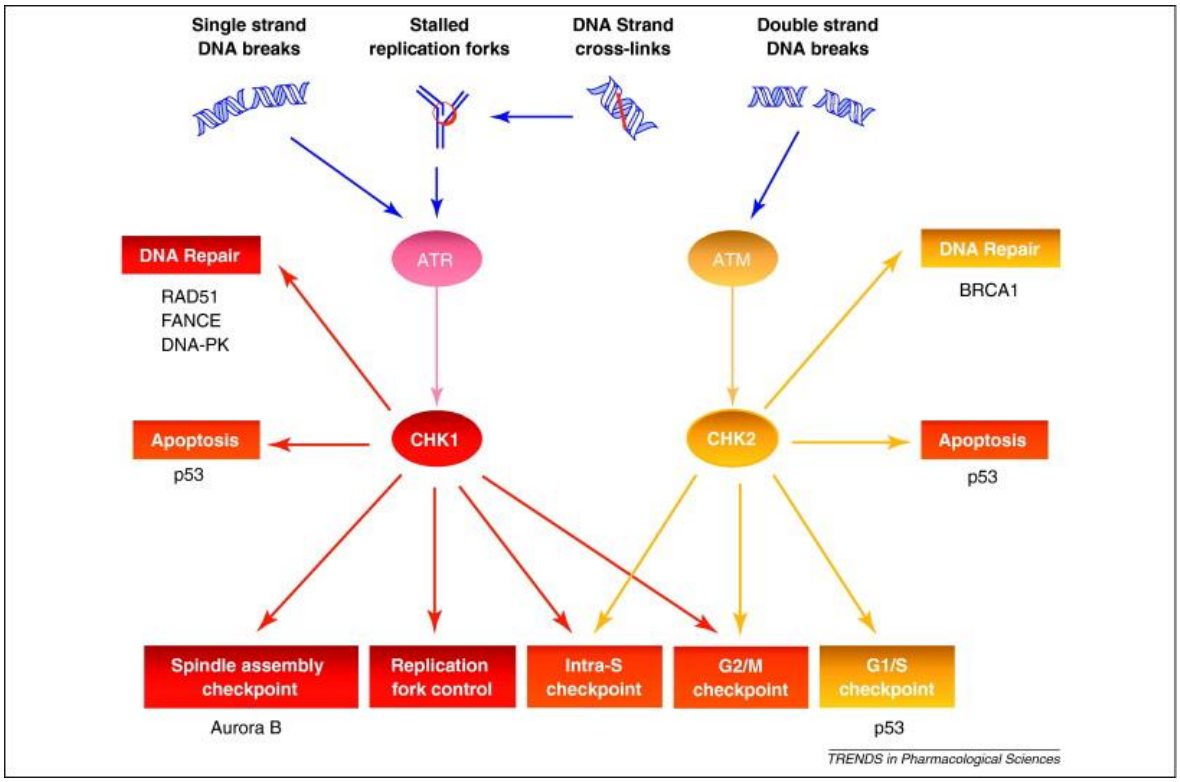

Figure 1.3. The DNA Damage Response (Garrett and Collins, 2011).

1.6.3 Inhibitors of CHK1/CHK2

Currently, there are many novel small molecules in development to target components of the DDR pathway for the treatment of ovarian cancer. Many of these molecular targeted drug candidates have been identified through fragment-based screening and structure-based drug design. Prexasertib (LY2606368) is dual inhibitor of both CHK1 and CHK2. A phase 2 clinical study showed that the median progression free survival for patients treated with Prexasertib was 7.4 months (Lee *et al.*, 2018). SRA737 (CCT245737), is a selective inhibitor of CHK1 with an IC_{50} of 1.4 nM against CHK1. In addition, SRA737 exhibited >1,000-fold selectivity against CHK2 and CDK1 (Walton *et al.*, 2016).

It has been suggested that CHK1 inhibition can be used in the treatment of ovarian cancer cells overexpressing Cyclin E. About 20% of high-grade ovarian carcinomas overexpress Cyclin E. The overexpression of Cyclin E is associated with high levels of replication stress. It has been shown that ovarian cancer cells overexpressing Cyclin E are more proficient at homologous recombination repair, which might be necessary for the survival of cells overexpressing Cyclin E (Lee *et al.*, 2018). The checkpoint kinase CHK1 is a key regulator of DNA repair by homologous recombination (Sørensen *et al.*, 2005). As a result, CHK1 inhibition in cells overexpressing Cyclin E may induce synthetic lethality.

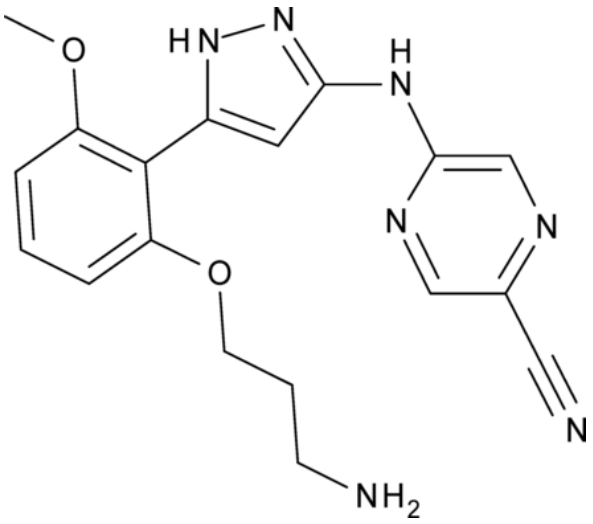

Kinase	IC_{50} (nM)
CHK1	< 1
CHK2	8

Figure 1.4. The Chemical Structure of Prexasertib (King *et al.*, 2015)**.**

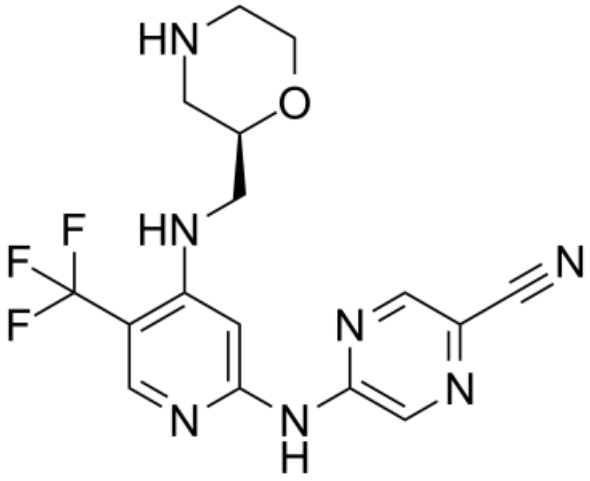

Kinase	IC_{50} (nM)
CHK1	1.4
CHK2	2440
CDK1	9030

Figure 1.5. The Chemical Structure of SRA737 (Walton *et al.*, 2016)**.**

1.3 Resistance to Cancer Therapies

A major problem in the treatment of ovarian cancer, and all other cancers, is the development of resistance. There are two forms of drug resistance; intrinsic resistance and acquired resistance. Intrinsically resistant cancer cells have the innate ability to resist cancer therapies and fail to respond to initial treatment (Lippert, Ruoff and Volm, 2011). Contrastingly, drug-resistant cancer cells can also develop as a result of repeated drug exposure. One way by which this can occur is by the selection of pre-existing drug-resistant cancer cells, by imposing a selection pressure such as drug treatment. Alternatively, it has also been suggested that 'drug tolerant' cells, that survive initial treatment due to epigenetic changes, undergo further evolution in order to acquire resistance mechanisms. For example, both of these mechanisms have been shown to play a role in the development of resistance to EGFR TKIs in non-small cell lung cancer (Hata *et al.*, 2016).

There are many mechanisms by which cancer cells may develop resistance to anti-cancer drugs which include, but are not limited to: efflux pumps, drug target alterations, drug target amplification, bypass of the drug target, activation of upstream or downstream signalling.

1.3.1 Efflux Pumps

A mechanism by which cancer cells develop resistance to anti-cancer drugs is via a number of transporter proteins that effect the accumulation of these drugs inside the cell. Multi-dug resistance (MDR) is described as the mechanism by which cancer cells develop resistance to structurally or functionally unrelated drugs (de Jong *et al.*, 2001). The adenosine triphosphate-binding cassette (ABC) transporter superfamily is an example of a class of cell membrane transporter proteins that alter the intracellular concentration of anti-cancer drugs by extruding these drugs from the cell as they travel down their concentration gradient. The most extensively characterised of these includes the ABCB1, which is also known as MDR1 or p-glycoprotein.(Fletcher *et al.*, 2010) Experiments have shown that decreased ABCB1 expression using siRNA can reverse Paclitaxel resistance in ovarian carcinoma cell lines (Duan, Brakora and Seiden, 2004).

1.3.2 Drug Target Alterations

The extent to which anti-cancer drugs are able to treat cancer is dependent upon the drugs target and modifications to this target which may include mutations or changes in the level of expression. Some of these modifications to the target may lead to the development of resistance to anti-cancer drugs. A mechanism by which cancer cells develop resistance to kinase inhibitors in particular is by altering the gate keeper residue, which alters the hydrophobic binding pocket giving limited access to the ATP competitive inhibitor. Gatekeeper mutations have been identified in non-small cell lung cancer patients resistant to Gefitinib. Structural analysis and biochemical studies revealed that these patients acquired Gefitinib resistance as a results of a second epidermal growth factor receptor (EGFR) point mutation, T790M (threonine-to-methionine mutation at codon 790 in EGFR) (Kobayashi *et al.*, 2005).

1.3.3 Drug Target Amplification

Amplification of the drug target is also a mechanism which cancer cells employ in order to confer resistance to many anti-cancer drugs, and it illustrates the dependency that these therapies have on drug target modifications. For example, whole exome sequencing has identified that amplification of the mutant B-RAF gene (V600E), and consequently B-RAF overexpression, confers resistance to the B-RAF inhibitor, Vemurafenib, in 20% of melanoma patients. It was also shown that B-RAF knockdown by shRNA confers sensitivity to Vemurafenib, supporting the idea that B-RAF inhibitor resistance develops as a result of a gain in (V600E) B-RAF copy number (Shi *et al.*, 2012).

1.3.4 Bypass of the Target Pathway

Pathway bypass is another mechanism which cancer cells have acquired to resist the effects of many anti-cancer drugs; it involves the recruitment of parallel pathways to re-engage the downstream signalling of the drug targeted pathway. For example, resistance to RAF- and MEK-inhibitors can develop in BRAF-mutant melanomas by activation of a GPCR signalling pathway. The signalling proceeds through adenylyl cyclase, protein kinase A and cAMP response element binding protein (CREB) to reactivate the transcription factors downstream of MAPK. Expression of these transcription factors also plays a role in RAF- and MEK inhibitor resistance (Johannessen *et al.*, 2013).

1.3.5 Activation of Upstream and Downstream Signalling

Cancer cells may acquire resistance by re-activating downstream components of the signalling pathway via effectors that lie upstream of the drug target. For example, it has been reported that resistance to B-RAF inhibitors can develop in B-RAF mutant-melanoma patients as a result of N-RAS overexpression. Activated N-RAS (Q61K), as a result of a mutation, signals to C-RAF over B-RAF to re-activate the MAPK pathway (Nazarian *et al.*, 2010). Alternatively, cancer cells may also acquire resistance by re-activating components of the signalling pathway that lie downstream of the drug target, irrespective of upstream signalling. For example, mutations in MEK1, both MEK1(P124L) and MEK1(Q56P) confer resistance to the B-RAF inhibitor, PLX4720 (Emery *et al.*, 2009).

1.4 Project Aims and Objectives

The aim of the project was to investigate potential mechanisms of acquired resistance to the CHK1 inhibitors, SRA737 and Prexasertib, in the human ovarian cancer cell line PEO1. Ovarian cancer cell lines with high cyclin E expression were identified using western blot analysis. Cell lines that overexpress cyclin E were selected and examined using the SRB proliferation assay to determine their sensitivity to the CHK1 inhibitors, SRA737 and Prexasertib. Based on this data, cells were treated with increasing concentrations of SRA737 or Prexasertib for a period of 6 months to generate resistant cell lines. Having generated resistant cell lines, the cells were profiled using inhibitors of ATR and ATM to confirm which part of the DDR pathway was responsible for resistance. The expression of these targets was further validated using western blot analysis.

2.0 Materials and Methods

2.1 Drugs and Compounds

Stock solution of SRA737 (Sierra Oncology, Canada), Prexasertib, AZD6738 (both AdooQ Biosciences, USA), AZD0156 (Selleck Chemicals, USA) were all prepared in DMSO (Sigma Aldrich, Germany). Stock solutions of Cisplatin (1 mg/ml) were prepared in 0.9% (w/v) saline (Sigma Aldrich).

2.2 Cell Lines and Culture

2.2.1 Routine Cell Culture

The EFO-27, EFO-21 and COLO-704 cell lines were obtained from DSMZ (Braunscheig, Germany), and the PEO1 and A2780 cell lines were obtained from ATCC (Virginia, USA). The EFO-27 and EFO-21 cells lines were cultured in Iscoves Modified Dulbecco's Medium (IMDM; Fisher Scientific), and the PEO1 and A2780 cell lines were cultured in Rosewell Park Memorial Institute (RPMI; Sigma Aldrich) 1640. Both cell culture mediums were supplemented with 10% foetal bovine serum (FBS; Sigma Aldrich). All cell lines were maintained at 37ºC in a humidified atmosphere of 5% CO_2 and passaging was performed on cells at 70% confluence. During passage, cells were washed with phosphate-buffered saline (PBS) and detached by incubation with Trypsin-EDTA (Sigma Aldrich). The cells were resuspended in media and transferred to a new tissue culture flask using an appropriate ratio. The COLO-704 cell line was provided as a cell pellet.

2.2.2 Generation of SRA737- and Prexasertib-Resistant Cell Lines

Cells were seeded into T25 tissue culture flasks and allowed to adhere overnight. The cells were then treated with SRA737 or Prexasertib at a concentration of 1XGI_{50}. The GI_{50} represents the concentration at which maximal growth is inhibited by 50% in a 96-hour SRB assay. Confluent cells were passaged and treated with an increased concentration of inhibitor. The inhibitor concentration was incrementally increased in multiples of the GI_{50}. This process was repeated for a period of 6 months, or until the resistance levels were at least 2-fold that of the parental cell line.

2.3 Characterisation of Cell Line Growth

2.3.1 Cell Seeding Density Assay

Cells were seeded into seven 96-well plates at densities ranging from 1,600-to-25,600 cells per well. Every 24 hours, a plate was fixed with 10% (w/v) trichloroacetic acid (TCA) and incubated at room temperature for 30 minutes. The plate was then washed 5 times with distilled water, before being stained with 0.4% (w/v) Sulforhodamine B (SRB) in 1% acetic acid and incubated at room temperature for 30 minutes. The cells were then washed 5 times with 1% acetic acid and dried overnight at 37ºC. The bound dye was solubilised in 10mM Tris, and each plate placed on an orbital shaker at 200rpm for 10 minutes. The Victor X4 Multilabel plate reader (PerkinElmer Life Sciences) was used to measure the absorbance of the solubilised dye at 490nm.

2.3.2 SRB Proliferation Assay

The SRB assay was used to determine the cells' sensitivity to several cytotoxic agents. Cells were seeded into a 96-well plate at the optimum density and allowed to adhere for 48 hours. The cytotoxic agents were serially diluted and added to the cells at the concentrations indicated. After a 96-hour incubation period, the cells were fixed and stained as above, and the absorbance measured at 490nm. The GI_{50} values were calculated using GraphPad Prism 6 (GraphPad Software Inc).

2.4 Cell Lysis and Western Blotting

2.4.1 Cell Lysis

Cells were plated into 10 cm dishes at an appropriate cell density and allowed to adhere for 48-72 hours. The media was aspirated, and the cells washed twice with ice-cold PBS. The cells were lysed and scraped with 70µl ice-cold lysis buffer (50mM HEPES pH 7.4, 250mM NaCl, 0.1% Nonidet-P40, 1mM DTT, 1mM EDTA pH 8.0, 1mM NAF, 10mM β-glycerophosphate, 0.1mM sodium orthovanadate and Complete™ protease inhibitor cocktail [Roche, Switzerland]). The cell lysates were transferred to 1.5ml Eppendorf tubes and incubated on ice for 30 minutes. The lysates were centrifuged at 14,000 rpm for 10 minutes at 4°C, and the supernatant aliquoted into clean 1.5ml Eppendorf tubes. The supernatant was kept on ice for subsequent use, or snap-frozen in dry-ice and stored at -80°C.

2.4.2 Protein Concentration Determination

The protein concentration of the cell lysates was determined using the Bradford assay. The BSA standards were made by diluting a 1mg/ml bovine serum albumin (BSA) stock solution to a working range of 0-500µg/ml (Table 1). The cell lysates were diluted 1:5, 1:10 and 1:20 with dH_20. The diluted BSA standards and cell lysates were then added in triplicate to a 96-well plate. The Bradford reagent (Bio-Rad) was diluted 1:5 with dH_20, and 200µl of the diluted reagent was added to each well. The plate was placed on an orbital shaker for 30 seconds at 200 rpm and incubated at room temperature for 5 minutes. The absorbance was read on the Victor X4 Multilabel Plate Reader (PerkinElmer Life Sciences, USA) at 595nm. The protein concentration of the cell lysates was determined using the BSA standard curve.

Table 1. Preparation of Diluted BSA Standards

Volume of Diluent (µL)	Volume of 1mg/ml BSA (µL)	Final BSA Concentration (µg/ml)
250	250	500
300	200	400
350	150	300
400	100	200
450	50	100
475	25	50
500	0	0

2.4.3 SDS-PAGE and Western Blotting

The samples were normalised, using 5x sample buffer as the diluent, to the lowest lysate concentration and heated at 95^{o}C for 5 minutes. Samples were equally loaded and run on 8-12% polyacrylamide gels in 1X running at 150V for 60-90 minutes. The PageRuler Plus Prestained Protein markers were used to allow for identification of protein size. Proteins were transferred to methanol activated PVDF membranes (Millipore, USA) in 1X transfer buffer at 100V for 90 minutes. The efficiency of the transfer was assessed by Ponceau S staining. Membranes were blocked in 5% (v/v) powdered milk (Marvel) in 1X TBST for 1 hour at room temperature and incubated with primary antibody in 5% Marvel/TBST overnight at 4^{o}C. Membranes were washed in 1X TBST for 2X10 minutes, before being incubated with secondary antibody in 5% Marvel/TBST for 1 hour at room temperature and washed in 1XTBST for a further 4X5 minutes. Proteins were visualised by exposure to Amersham Hyperfilm ECL following incubation with Pierce ECL western blotting substrate for 5 minutes at room temperature. Blots were developed using the developer and scanned on the Optimax 2010 x-ray processing machine. Membranes were washed in stripping buffer for 2X5 minutes and re-probed with a different primary antibody.

Table. 2. List of Buffer/Solutions used for Western Blotting

Buffer/Solution	Reagents	pH
Running Buffer (10x)	0.25M Tris-HCl, 1.92M Glycine, 1% SDS	N/A
Transfer Buffer (10x)	0.25M Tris-HCl, 1.92M Glycine	N/A
TBS (10x)	50mM Tris-HCl, 150mM NaCl	8.0
TBST	50mM Tris-HCl, 150mM NaCl, 0.1% Tween-20	N/A
Sample Buffer (5x)	1.5M Tris (pH 6.8), 50% glycerol, 25% β-mercaptoethanol, 1% SDS, 5% (1%)-bromophenol blue	N/A
Stripping Buffer	50mM Glycine, 1% SDS	2.0
Stacking Buffer	0.5M Tris-HCl, 0.4% SDS	6.8
Resolving Buffer	1.5M Tris-HCl, 0.4% SDS	8.8

Table. 3. List of Primary Antibodies used for Western Blotting

Primary Antibody	Dilution	Catalogue#	Source	Species
Cyclin E	1:1000	sc-377100	Santa Cruz Biotechnology, Inc.	Mouse
Cyclin A	1:1000	sc-271682	Santa Cruz Biotechnology, Inc.	Mouse
Cyclin D	1:1000	sc-20044	Santa Cruz Biotechnology, Inc.	Mouse
Cyclin B	1:1000	sc-245	Santa Cruz Biotechnology, Inc.	Mouse
pCHK1	1:500	2349S	CST	Rabbit
tCHK1	1:1000	2360S	CST	Mouse
pCHK2	1:500	2669T	CST	Rabbit
tCHK2	1:1000	6334S	CST	Rabbit
pCDK1	1:2000	9111S	CST	Rabbit
tCDK1	1:2000	sc-8395	Santa Cruz Biotechnology, Inc.	Mouse
γH2AX	1:500	JBW301	Merck	Rabbit
WEE1	1:1000	sc-525285	Santa Cruz Biotechnology, Inc.	Mouse
p21	1:1000	2947S	CST	Rabbit
GAPDH	1:100K	MAB374	Merck	Mouse

Table. 4. List of Secondary Antibodies used for Western Blotting

Secondary Antibody	Dilution	Catalogue#	Source	Species
Anti-mouse HRP conjugate	1:10K	170-6516	Bio-Rad	Goat
Anti-rabbit HRP conjugate	1:10K	170-6515	Bio-Rad	Goat

3.0 Results

3.1 Introduction

The CCNE1 gene, which encodes the protein cyclin E, is amplified in 20% of primary high grade-ovarian carcinomas. The amplification of CCNE1 is associated with the development of chemotherapeutic resistance. It has also been shown that overexpression of cyclin E is associated with high levels of replication stress. A recent study revealed that cancers with CCNE1 amplification are more proficient at homologous recombination. As a result, cancers overexpressing cyclin E might have a greater dependency on homologous recombination for survival (Lee *et al.*, 2018). The checkpoint kinase CHK1 is a key regulator of DNA repair by homologous recombination (Sørensen *et al.*, 2005). Therefore, cancers with cyclin E overexpression might show greater sensitivity to CHK1 inhibition. The CHK1 inhibitors SRA737 and Prexasertib are currently being clinically evaluated in ovarian cancer patients (Walton *et al.*, 2016) (Lee *et al.*, 2018).

3.2 Identification and Characterisation of the Parental Cell Line

Initially, five ovarian cancer lines were characterised according to Cyclin E expression, growth characteristics and drug response to SRA737 and Prexasertib. The cell lines studied were EFO-27, EFO-21, A2780, PEO1 and COLO-704. The majority of the cell lines grew as an adherent monolayer, except COLO-704, which grows as a suspension culture. The cell lines were all morphologically distinct (Figure 3.1.)

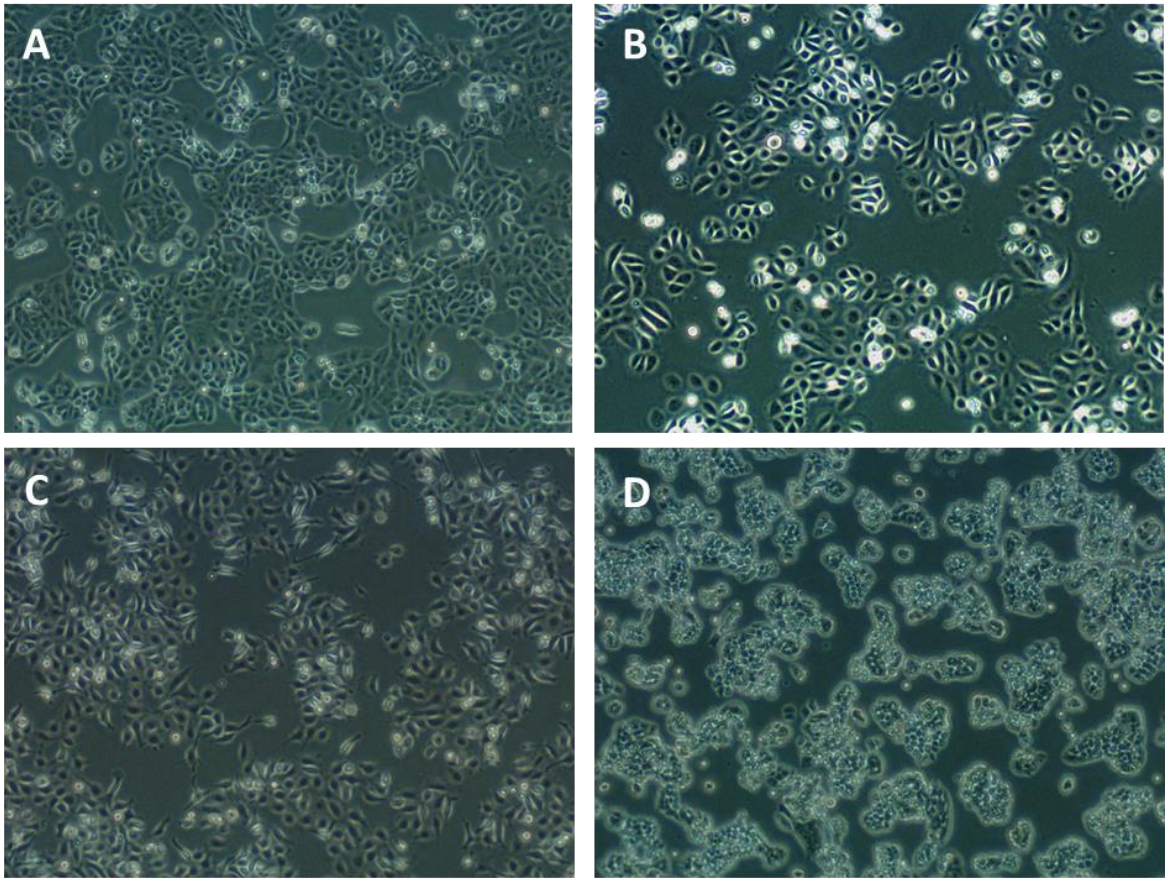

Figure. 3.1. Brightfield Microscopy Images of Ovarian Cancer Cell Lines in Culture. Images of (A) PEO1, (B) EFO-21, (C) EFO-27, and (D) A2780 cells at 50x magnification. Images were taken using the Olympus CKX53 microscope. COLO-704 not shown.

3.2.1 Analysis of Cyclin E Expression in Ovarian Cancer

Expression of Cyclin E was examined by western bot analysis (Figure. 3.2.). The PEO1 cells were shown to express the highest levels of Cyclin E. However, the A2780 cells were also found to overexpress Cyclin E. Cyclin E expression was relatively consistent between the EFO-27, EFO-21 and COLO-704 cells.

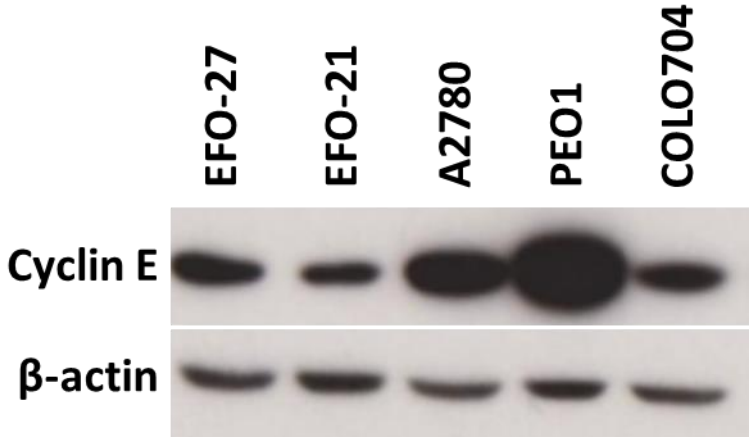

Figure. 3.2. Western Blot Analysis of Cyclin E Expression. Cyclin E expression was detected by western blot analysis as described in the materials and methods with 26µg protein loaded per lane. β-actin was used as a loading control. Similar results were obtained in repeated experiments.

3.2.2 Growth Characterisation of the PEO1 Cell Line

The PEO1 cells overexpressing Cyclin E were selected and further examined using the SRB proliferation assay (Figure 3.3.). The SRB assay was used to determine the optimum cell density which ensures logarithmic growth for the duration of a 96-hour SRB assay. The optimum cell density is required before carrying out GI_{50} determinations, this is to ensure that the observed response is due to the action of the CHK1 inhibitor rather than as a result of contact inhibition by the cells. Contact inhibition is where neighbouring cells contact one another and undergo cell cycle arrest. Cells were seeded at five different densities into seven 96-well plates. A plate was fixed every 24 hours before being stained with SRB. After being washed out and dried, the bound dye was solubilised and the absorbance of the solubilised dye measured at 490nm. The growth curves show that the optimum seeding density for the cell line PEO1 is 6400 cells per well, as this density permitted logarithmic growth between 48 and 144 hours. The doubling time for the PEO1 cells was calculated to be approximately 37.4 hours.

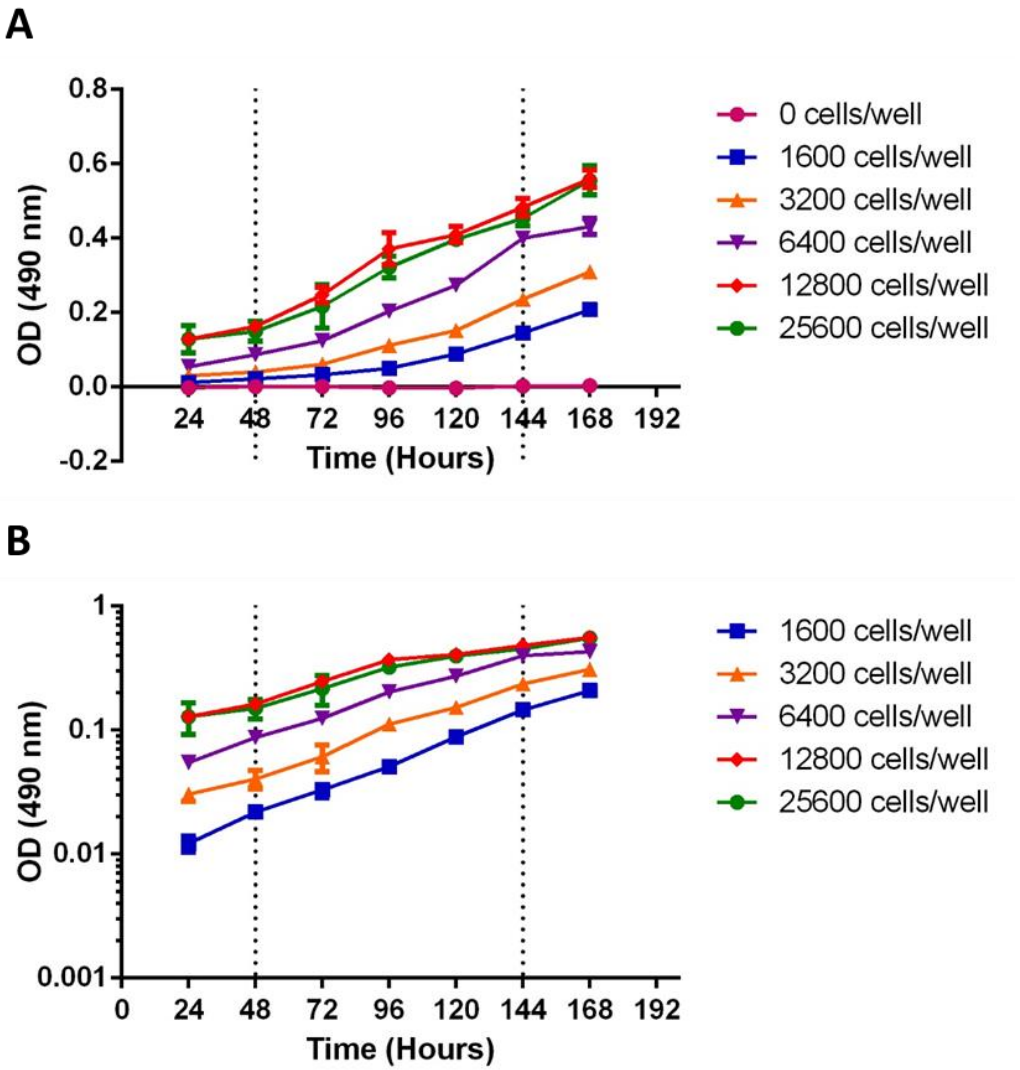

Figure. 3.3. Growth Characteristics of the PEO1 Parental Cell Line. PEO1 cells were seeded at the densities shown and incubated at 37°C in a humidified atmosphere of 5% CO_2. Cells were fixed and stained at 24, 48, 72, 96, 120, 144 and 168 hours, as described in the materials and methods, and the absorbance was measured at 490nm. Linear absorbance (A) and logarithmic absorbance (B) versus time. Data representative of n=3 biological repeats.

3.2.3. The Response of PEO1 Cells to SRA737 and Prexasertib

The SRB assay was used to measure the response of PEO1 cells to SRA737 and Prexasertib. Cells were seeded into a 96-well plate at the optimum density of 6400 cells per well. The cells were treated with multiple concentrations of either SRA737 or Prexasertib. After a 96-hour incubation period, the plate was fixed, stained with SRB, washed and dried, the bound dye solubilised and the absorbance of the solubilised dye measured at 490nm. The response was quantified by calculating the GI_{50} value, which represents the concentration at which maximal growth is reduced by half. The GI_{50} values for SRA737 and Prexasertib were 0.31µM and 12.09nM, respectively (Figure 3.4.). These values indicate that the PEO1 cell line is more sensitive to Prexasertib than it is to SRA737.

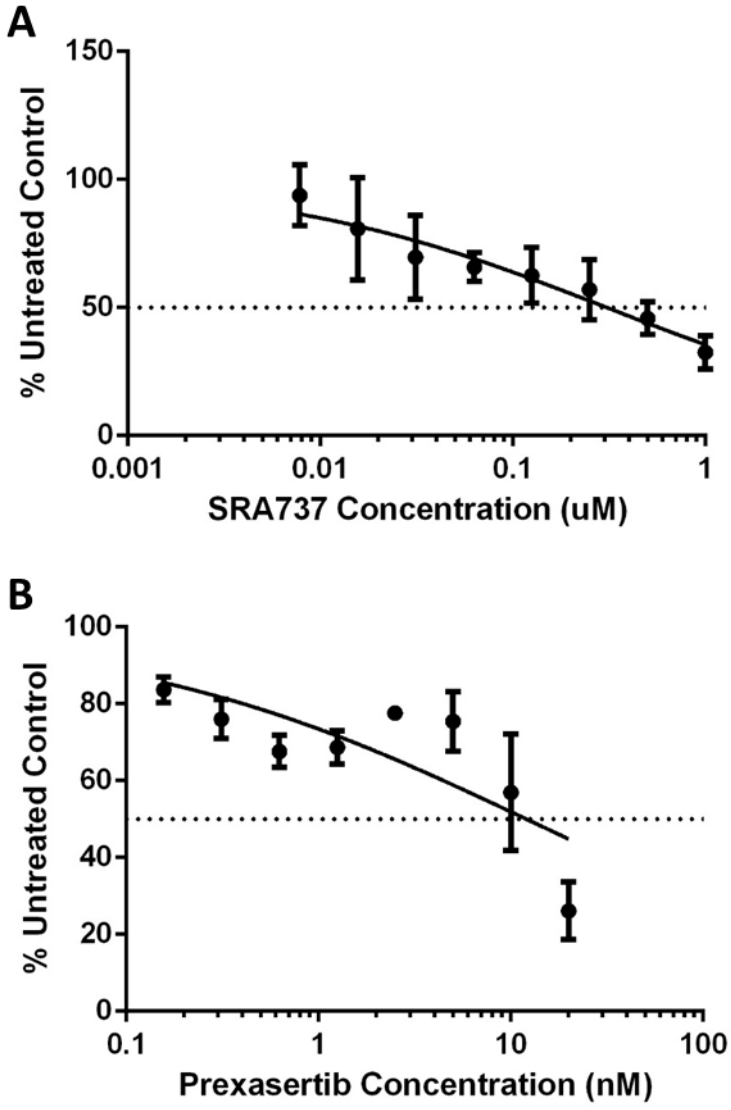

Figure. 3.4. Dose-Response Analysis of PEO1 Cells to (A) SRA737 and (B) Prexasertib. Cells were seeded at the optimum density into a 96-well plate and treated with multiple concentrations of SRA737 and Prexasertib. The dose response curves were analysed using GraphPad Prism 6. The data points represent mean±SD.

3.3 Generation and Characterisation of the SRA737- and Prexasertib-Resistant Cell Lines

3.3.1 Generation of the SRA737- and Prexasertib-Resistant Cell Lines

The resistant cell lines were generated using a method known as dose escalation. To start with, the cells were cultured in the presence of inhibitor at a concentration of 1xGI_{50}. When 70% confluency was reached, the cells were passaged and treated with a higher concentration of inhibitor. The concentration of inhibitor was increased incrementally in multiples of the GI_{50}. The GI_{50} value for each of the resistant cell lines was taken at regular intervals to monitor the fold change in resistance with respect to the parental cell line. The resistant cell lines were generated over a period of six months, or until the corresponding RF was twice that of the parental cell line. The incremental increase in inhibitor concentration during the development of the resistant cell lines can be seen in Figure 3.5. Furthermore, the resistant cell lines were maintained in a heterogeneous population opposed to isolated into individual resistant sub-clones. The SRA737- and Prexasertib-resistant cell lines were named PEO1737 and PEO1PREX, respectively.

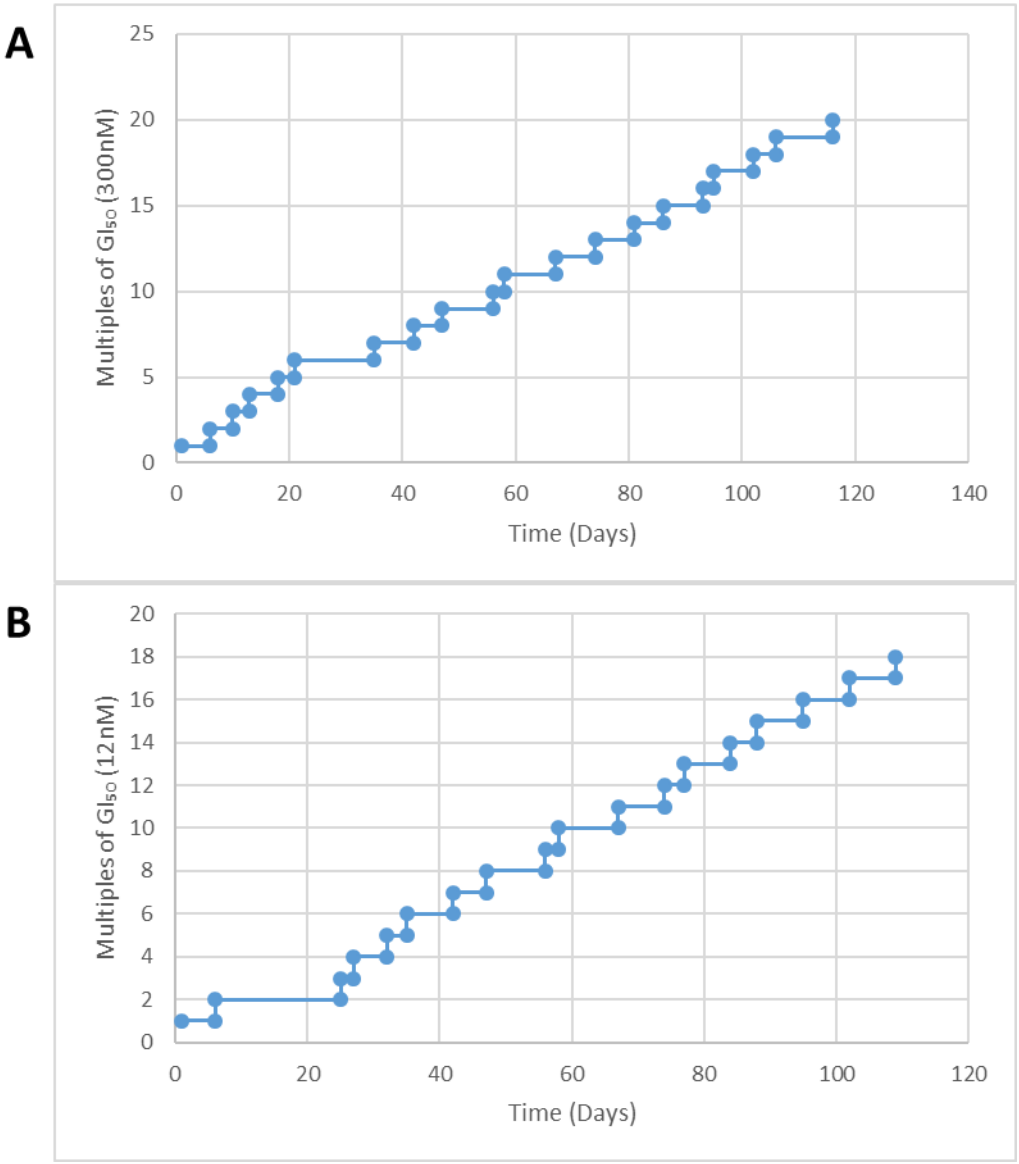

Figure. 3.5. Generation of the (A) SRA737- and (B) Prexasertib Resistant Cell Lines. The incremental increase in inhibitor concentration during the development of the resistant cell lines. The inhibitor concentration was increased in multiples of the GI_{50}.

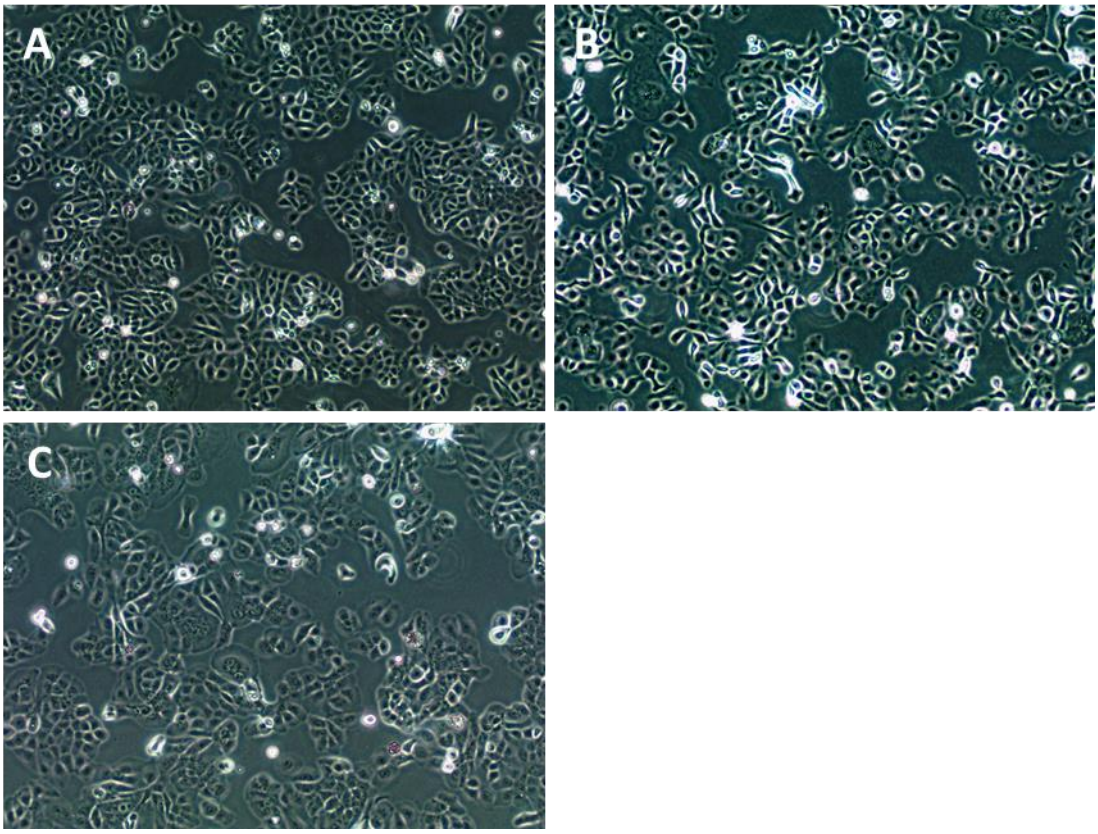

Figure. 3.6. Brightfield Microscopy Images of the SRA737- and Prexasertib-Resistant Cell Lines in Culture. Images of (A) PEO1P, (B) PEO1737, (C) PEO1PREX cells at 50x magnification. Images were taken using the Olympus CKX53 microscope.

3.3.2 Growth Characteristics of SRA737- and Prexasertib-Resistant Cell Lines

The SRB assay was used to determine whether the growth rate of the resistant cell lines had changed with respect to the parental cell line. The SRA737- and Prexasertib-resistant cell lines grew at a similar rate to the parental cell line, with doubling times of 31.5- and 32.5-hours, respectively. However, the optimum seeding density for the resistant cell lines was 3,200 cells per well, half that of the parental cell line (Figures 3.7. and 3.8.).

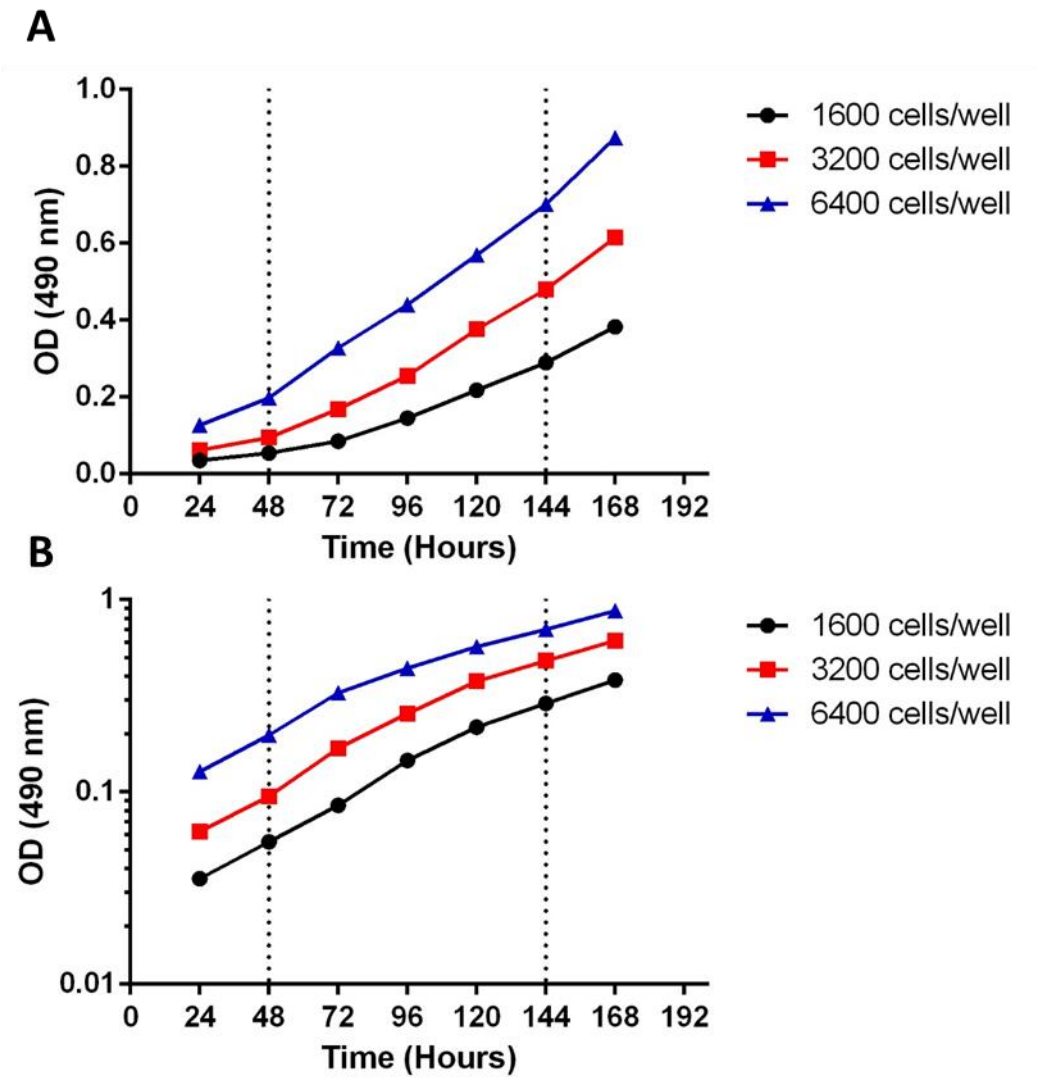

Figure. 3.7. Growth Characteristics of the SRA737-Resistant Cell Line. PEO1737 cells were seeded at the densities shown and incubated at 37°C in a humidified atmosphere of 5% CO_2. Cells were fixed and stained at 24, 48, 72, 96, 120, 144 and 168 hours, as described in the materials and methods, and the absorbance was measured at 490nm. Linear absorbance (A) and logarithmic absorbance (B) versus time. Data representative of n=2 biological repeats.

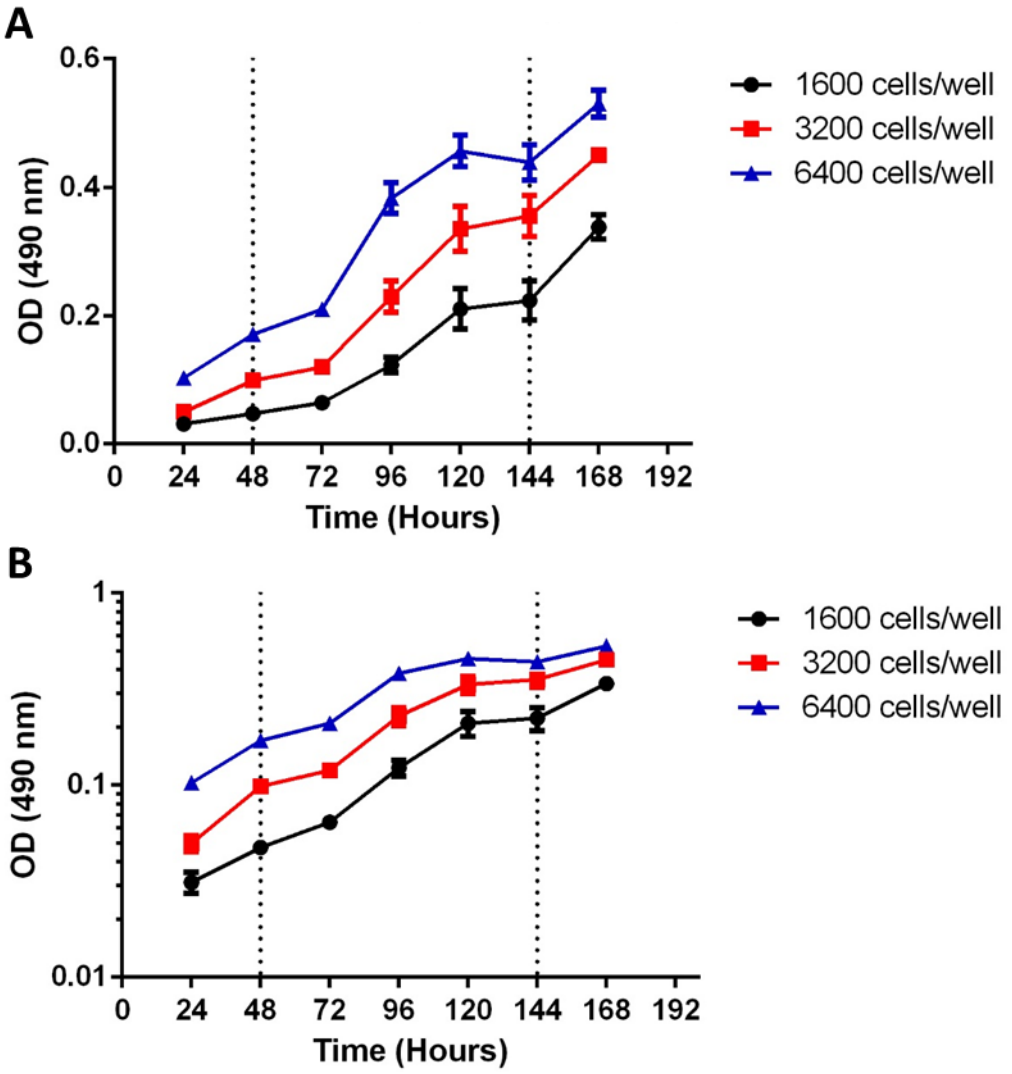

Figure. 3.8. Growth Characteristics of the Prexasertib-Resistant Cell Line. PEO1PREX cells were seeded at the densities shown and incubated at 37°C in a humidified atmosphere of 5% CO_2. Cells were fixed and stained at 24, 48, 72, 96, 120, 144 and 168 hours, as described in the materials and methods, and the absorbance was measured at 490nm. Linear absorbance (A) and logarithmic absorbance (B) versus time. Data representative of n=2 biological repeats.

3.3.3. GI_{50} Determination of SRA737- and Prexasertib Resistant Cell Line

The SRB assay was used to determine the GI_{50} value for each of the CHK1 inhibitors in each of the resistant cell lines. The GI_{50} value obtained was then be used to calculate the resistance factor. The resistance factor (RF) represents the fold change in the GI_{50} for each of the resistant cell lines compared to that of the parental cell line. It is a method of quantifying the level of resistance generated in each of the resistant cell lines as a result of dose escalation. The RF can be calculated as a ratio of resistant GI_{50} to parental GI_{50}.

$$Resistance\ Factor\ = \frac{Resistant\ GI_{50}}{Parental\ GI_{50}}$$

The growth curves show a shift in the GI_{50} value for both the CHK1 inhibitors in each of the resistant cell lines, indicating not only the generation of resistance, but the generation of cross-resistance to each of the CHK1 inhibitors (Figure. 3.9.). The calculated RF for SRA737 and Prexasertib in the SRA737-resistant cell line was 2.46 and 2.56, respectively. In the Prexasertib-resistant cell line, the calculated RF was 225.84 for SRA737 and 338.17 for Prexasertib. The RFs and corresponding GI_{50} values for the CHK1 inhibitors in the resistant cell lines have been summarised in Table 5.

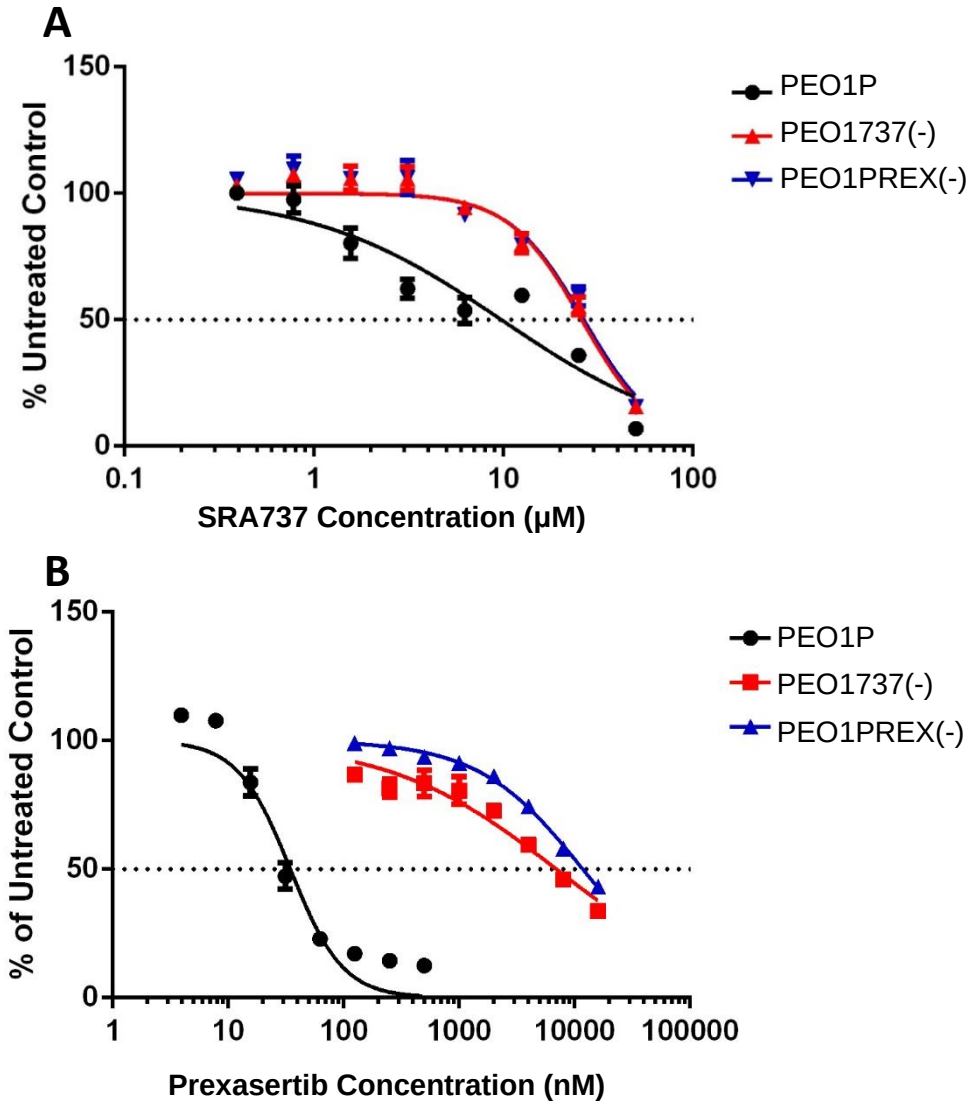

Figure. 3.9. Dose-Response Analysis PEO1 Parental and Resistant Cell Lines to (A) SRA737 and (B) Prexasertib. Cells were seeded at the optimum density into a 96-well plate and treated with multiple concentrations of SRA737 and Prexasertib. The dose response curves were analysed using GraphPad Prism 6. The data points represent mean±SD. Data representative of n=3 biological repeats.

Table. 5. Resistance Profiling of PEO1 Cells to CHK1 inhibition. Summary of GI_{50} values and resistance factors for both SRA737 and Prexasertib in the PEO1 parental and resistant cell lines. Data obtained represents n=3 independent experiments. Students T-test* P ≤0.05

PEO1		Cell Line											
		Parental				SRA737 Resistant				Prexasertib Resistant			
Drugs	Target	GI_{50}±SD GraphPad (µM)	GI_{50}±SD Calcusyn (µM)	R^2 Value	n No.	GI_{50}±SD (µM)	RF (GraphPad)	RF (Calcusyn)	n No.	GI_{50}±SD (µM)	RF (GraphPad)	RF (Calcusyn)	n No.
SRA737	CHK1	10.12±2.56	12.92±7.6	0.87	3	24.92±2.79	2.46*	1.93	n=3	25.74±1.56	2.54*	1.99	3
Prexasertib	CHK1/2	0.035±0.0004	N/A	N/A	3	7.79±0.95	225.84*	N/A	n=3	11.67±0.77	338.17*	N/A	3

The parental cell lines did not have the same response to SRA737 and Prexasertib as previously measured before the dose escalation was initiated (Figure 3.4.). The GI_{50} values for SRA737 and Prexasertib in the parental cell line increased 33- and 3- fold, respectively. In addition, the parental cell line did not respond to SRA737 in the same way as Prexasertib. Cell viability was found to decrease linearly in response to increasing concentrations of Prexasertib. In contrast for SRA737, cell viability plateaued at approximately 50% between 3.1µM and 12.5µM, and then decreased further as the concentration of SRA737 increased. Calcusyn was used to calculate the exact SRA737 concentration at which cell viability crosses 50%. The GI_{50} value for SRA737 in the parental cell line was 12.92 µM. However, the GraphPad values were used to describe the fold change in the GI_{50} given that the relationship between cell viability and SRA737 concentration had an R^2 value of 0.87 (Table 5).

3.3.4 Cross-Resistance to ATR and ATM Inhibition

The serine/threonine protein kinases ATR and ATM are key regulators of the DNA damage response pathway. To elucidate where along the signalling pathway resistance was occurring, cross-resistance profiling was performed using ATR inhibitor AZD6738 and the ATM inhibitor AZD0156 (Figure 3.10.). In both the resistant cell lines, cross-resistance was observed to the ATR inhibitor. The Prexasertib-resistant cell line is more resistant to AZD6738 than the SRA737-resistant cell line. The calculated RF for AZD6738 in the SRA737- and Prexasertib-resistant cell line was 5.85 and 11.95, respectively. Contrastingly, both the resistant cell lines showed a limited sensitivity to the ATM inhibitor, AZD0156. The RF for AZD0156 was 0.65 in the SRA737-resistant cells and 0.69 in the Prexasertib-resistant cells, indicating a similar level of sensitivity between the two resistant cell lines. A summary of the RFs and corresponding GI_{50} values for both AZD6738 and AZD0156 in the PEO1 parental and resistant cell lines can be found in Table 6.

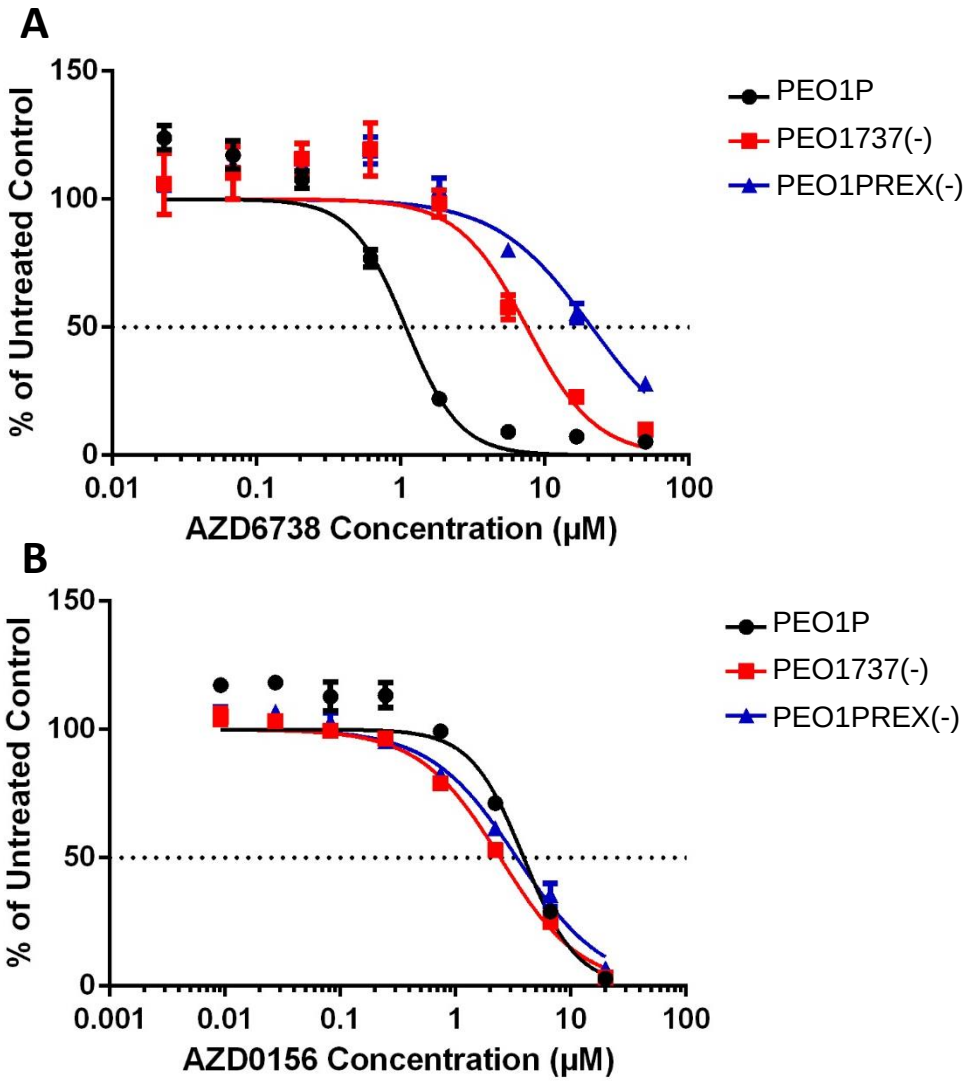

Figure. 3.10. Cross-resistance Profiling of PEO1 Cell Lines to (A) ATR and (B) ATM Inhibition. Cells were seeded at the optimum density into a 96-well plate and treated with multiple concentrations of AZD6738 and AZD0156. The dose response curves were analysed using GraphPad Prism 6. The data points represent mean±SD. Data representative of n=2 biological repeats.

Table. 6. Cross-resistance Profiling of PEO1 Cell Lines to ATR and ATM Inhibition. Summary of GI_{50} values and resistance factors for both AZD6738 and AZD0156 in the PEO1 parental and resistant cell lines. Data obtained represents n=3 independent experiments. Student's T-test * P ≤0.05

PEO1		Cell Line							
		Parental		SRA737 Resistant			Prexasertib Resistant		
Drugs	Target	GI_{50}±SD GraphPad (μM)	n No.	GI_{50}±SD GraphPad (μM)	RF (GraphPad)	n No.	GI_{50}±SD GraphPad (μM)	RF (GraphPad)	n No.
AZD6738	ATR	1.21±0.41	3	7.08±1.71	5.85*	3	14.56±5.73	11.95*	3
AZD0156	ATM	3.75±0.16	3	2.45±0.08	0.65*	3	2.6±0.71	0.69	3

3.3.5 Basal Western Blots of the Parental and Resistant Cell Lines

Western blot analysis was used to investigate the changes in basal signalling in the SRA737- and Prexasertib-resistant versus the parental cell line. Phosphorylated CHK1 was not detected in any of the three cell lines. The total amount of CHK1 remained unchanged in the resistant cell lines with respect to the parental cell line. The levels of phosphorylated CHK2 remained relatively consistent in both the parental and resistant cell lines. The total amount of CHK2 was higher in the resistant cell lines compared to the parental cell line (Figure 3.11). All the cyclins were upregulated in the resistant cell lines when compared to the parental cell line. The levels of p21 and WEE1 were also higher in the resistant cell lines when compared to the parental cell line. The levels of phosphorylated CDK1 (Y15) were similar in both the parental and drug resistant cell lines. The total amount of CDK1 remained unchanged in the resistant cell lines with respect to the parental cell line (Figure 3.12).

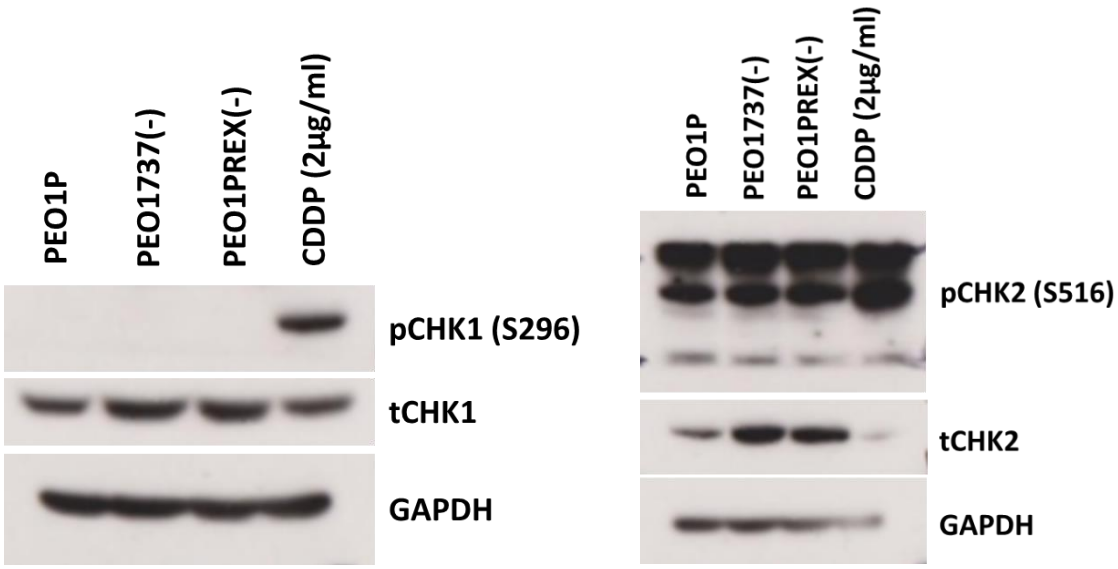

Figure. 3.11. Basal Western Blots of the SRA737- and Prexasertib-Resistant Cell Lines Versus the Parental Cell Line. CHK1 and CHK2 proteins were detected by western blot analysis as described in the material and methods with 52.4µg protein loaded per lane. GAPDH was used as a loading control, and PEO1 cells treated with 2µg/ml Cisplatin for 24 hours were used as a CHK1 positive control.

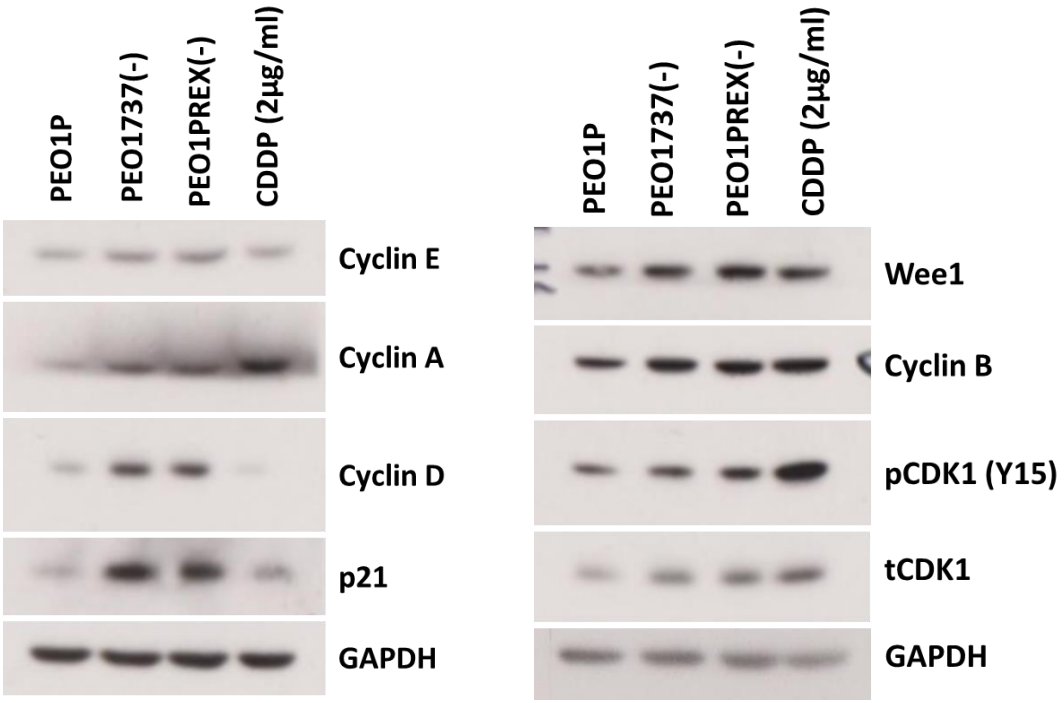

Figure. 3.12. Basal Western Blots of the SRA737- and Prexasertib-Resistant Cell Lines Versus the Parental Cell Line. CHK1/CHK2 signalling proteins were detected by western blot analysis as described in the material and methods with 56.2µg protein loaded per lane. GAPDH was used as a loading control, and PEO1 cells treated with 2µg/ml Cisplatin for 24 hours were used as a CHK1 positive control.

3.3.6 Dose-Response of Parental and Prexasertib-Resistant Cell Lines to Prexasertib

Western blot analysis was used to investigate the changes in CHK1 signalling in the parental versus the Prexasertib-resistant cell line in response to increasing concentrations of Prexasertib. (Figure. 3.13.). Prexasertib induced the phosphorylation of CHK1 (S345) in both the parental and Prexasertib-resistant cell lines. The levels of phosphorylated CHK1 (S345) remained relatively consistent in the parental and Prexasertib-resistant cell line in response to increasing concentrations of Prexasertib, however lower levels of phosphorylated CHK1 were present in the Prexasertib-resistant cell line when compared to the parental cell line. The total amount of CHK1 decreased in response to increasing concentrations of Prexasertib in both the parental and Prexasertib-resistant cell line. The levels of phosphorylated CDK1 (Y15) decreased in the Prexasertib-resistant cell line and remained relatively consistent in the parental cell line in response to increasing concentrations of Prexasertib. The total amount of CDK1 remained relatively consistent in both the parental and Prexasertib-resistant cell line in response to increasing concentrations of Prexasertib. The levels of p21 decreased in the Prexasertib-resistant cell line, whereas in the parental cell line they remained relatively consistent in response to increasing concentrations of Prexasertib. The levels of Wee1 remained relatively consistent in the Prexasertib-resistant cell line, whereas in the parental cell line the levels of Wee1 decreased in response to increasing concentrations of Prexasertib. There was strong induction of γH2AX in the parental cell line in response to increasing concentrations of Prexasertib, but very limited induction on the Prexasertib-resistant cell line.

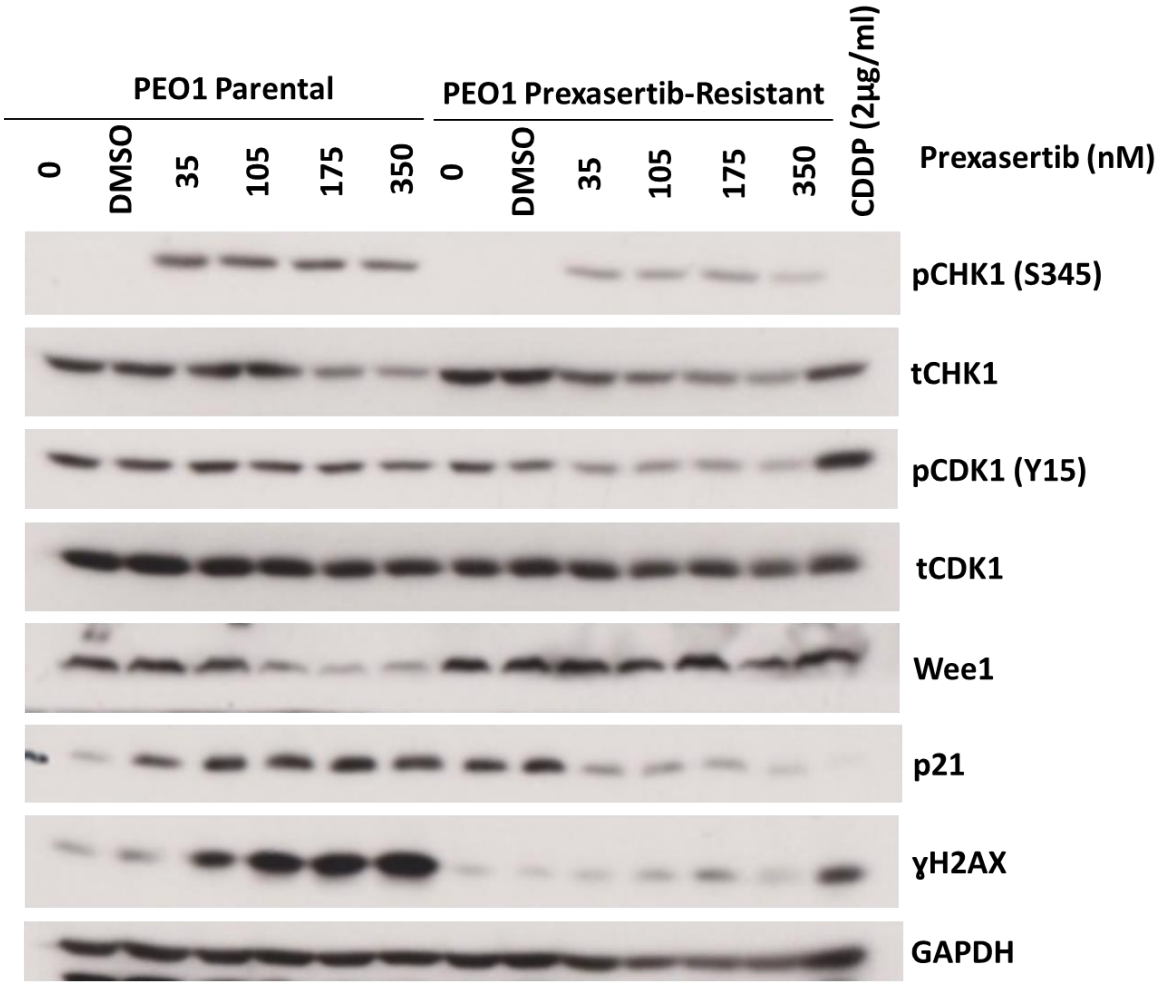

Figure. 3.13. Dose-Response Western Blot Analysis of Prexasertib in the Parental and Prexasertib-Resistant Cell Lines. Phosphorylated CHK1 (S345) and total CHK1, along with selected proteins downstream of CHK1, were detected by western blot analysis as described in the material and methods with 50µg protein loaded per lane. Cells were incubated with various concentrations of Prexasertib for 24 hours prior to cell lysis. GAPDH was used as a loading control. PEO1 cells treated with 2µg/ml Cisplatin for 24 hours were used as a CHK1 positive control. Data representative of n=3.

4.0 Discussion

4.1 Introduction

The primary aim of the project was to investigate the mechanisms of resistance to the CHK1 inhibitors, SRA737 and Prexasertib. The CHK1 inhibitors SRA737 and Prexasertib are currently being clinically evaluated in ovarian cancer patients (Walton *et al.*, 2016) (Lee *et al.*, 2018). The gene CCNE1, which encodes the protein Cyclin E, is amplified in approximately 20% of epithelial ovarian carcinomas. The overexpression of Cyclin E is associated with high levels of replication stress. Ovarian cancer cells overexpressing Cyclin E have been found to be more proficient at DSB repair by homologous recombination. Therefore, ovarian cancer cells overexpressing Cyclin E might have a greater dependency on homologous recombination repair for survival (Lee *et al.*, 2018). A major regulator of homologous recombination repair is the checkpoint kinase CHK1 (Sørensen *et al.*, 2005). As a consequence, ovarian cancer cells overexpressing Cyclin E may display a greater sensitivity to CHK1 inhibition.

4.2 Characterisation of the PEO1 Parental Cell Line

4.2.1 The Response of PEO1 Cell to SRA737 and Prexasertib

The SRB assay was used to measure the response of PEO1 cells to both SRA737 and Prexasertib (Figure 3.4.). It was found that PEO1 cells are significantly more sensitive to Prexasertib than they are to SRA737, with GI_{50} values of 12.09nM and 0.31µM, respectively. The PEO1 cells may be more sensitive to Prexasertib because it is a dual inhibitor of both CHK1 and CHK2. In comparison to SRA737, Prexasertib has a broader specificity profile which means the inhibitor can target multiple signalling pathways at once (Lee *et al.*, 2018). Also, it may be that the influx, efflux and metabolism rates of Prexasertib differ to that of SRA737.

4.3 Generation and Characterisation of the SRA737- and Prexasertib-Resistant Cell Lines

4.3.1 Generation of the SRA737- and Prexasertib-Resistant Cell Lines

The resistant cell lines were generated by a method known as dose escalation (Figure 3.5.). The resistance factors for SRA737 and Prexasertib in the SRA737-resistant cell line were 2.5 and 225.8, respectively. In contrast, the Prexasertib-resistant cell line achieved 2.6 and 338.2-fold resistance to SRA737 and Prexasertib, respectively (Table 5). Both resistant cell lines were more resistant to Prexasertib than they were to SRA737. One explanation for this might be that SRA737 has a relatively high starting GI_{50} compared to Prexasertib, and as a result those resistance mechanisms generated can only do so much to overcome the effects of SRA737 before the drug starts to have off target effects. Another explanation for this might be that the PEO1 cell line is effectively resistant to SRA737 to begin with. In one study the GI_{50} value for SRA737 ranged between 0.41µM and 5.4µM in the cell lines they looked at (Walton *et al.*, 2016). Given that we found the GI_{50} value for SRA737 to be 12.92µM, approximately 32-to-2-fold higher than that found by Walton *et al*, might suggest that the PEO1 cell line is already resistant to SRA737.

4.3.2 Growth Characteristics of the SRA737- and Prexasertib Resistant Cell Lines

The SRB assay was used to compare the growth rates of the parental versus the SRA737- and Prexasertib-resistant cell lines (Figure 3.7. and Figure 3.8.). The resistant cell lines had a similar growth rate to that of parental cell line. However, the optimum seeding density for the resistant cell lines was half that of the parental cell line at 3,200 cells per well. If the PEO1-resistant cells were larger than the PEO1-parental cells, then one might expect the resistant cell lines to reach contact inhibition at a cell density smaller than that of the parental cell line.

4.3.3 GI_{50} Determinations for the SRA737- and Prexasertib-Resistant Cell Lines

When conducting GI_{50} determinations for the resistant cell lines, the parental cell line did not respond to SRA737 and Prexasertib as previously measured before the dose escalation was initiated. The GI_{50} values for SRA737 and Prexasertib increased 33- and 3-fold, respectively (Figure 3.9.). The differences in the GI_{50} values suggest that the parental cell line is significantly less sensitive to CHK1 inhibition than previously reported (Figure 3.4.). It is more than likely that these differences are the result of experimental errors. For example, cell counting using a haemocytometer relies heavily upon visualisation. Visualisation can be impaired for a number of reasons including cell aggregation and debris. This can lead to variations in cell number that are not truly representative of the sample and consequently differences in GI_{50} values.

In addition, the parental cell line did not respond to SRA737 in the same way as Prexasertib. Cell viability was found to decrease linearly with respect to Prexasertib concentration. In contrast for SRA737, cell viability plateaued at approximately 50% between 3.1µM and 12.5µM, and then decreased further as the concentration of SRA737 increased (Figure 3.9.). The initial decline in cell viability may be the result of CHK1 inhibition, but at high concentrations SRA737 may start to have off target effects which would account for the second decline in cell viability. SRA737 is also a potent inhibitor of ribosomal protein S6 kinase (RSK1) with a 258-fold selectivity against RSK1 (Walton *et al.*, 2016). RSK1 is a key regulator of a number of cellular processes including cell invasion and metastasis (Ludwik *et al.*, 2016).

4.3.4. Cross-Resistance to ATR and ATM Inhibition

The parental and drug resistant cell lines were profiled using inhibitors of both ATR and ATM (Figure 3.10.). ATR and ATM are key regulators of the DNA damage response (DDR) pathway. Cross-resistance profiles can be used to predict candidate mechanism of resistance. The resistant cell lines were both found to be cross-resistant to the ATR inhibitor AZD6738. The Prexasertib-resistant cell line is more resistant to AZD6738 than the SRA737-resistant cell line with respect to the parental cell line. The RF for AZD6738 in the SRA737- and Prexasertib-resistant cell lines were 5.85 and 11.95, respectively. The fact that both the resistant cell lines are resistant to both CHK1 and ATR inhibition suggests that the resistance mechanism is independent of CHK1 activity, and that resistance may be being driven by a downstream target or an alternative signalling pathway.

The resistant cell lines both showed a slight sensitivity to the ATM inhibitor AZD0156. The RF for AZD0156 was 0.65 in the SRA737-resistant cell line and 0.69 in the Prexasertib-resistant cell line, this illustrates that there was a similar level of sensitivity to ATM inhibition in both of the resistant cell lines. The fact both the resistant cell lines display sensitivity to ATM inhibition may indicate that the resistance mechanism is being driven via the ATM-CHK2 branch of the DDR pathway. SRA737 and Prexasertib are two ATP-competitive inhibitors of CHK1. The fact that both the resistant cell lines display a similar level of sensitivity to ATM inhibition may suggest a common mechanism of resistance between each of the resistant cell lines.

4.3.5 Basal Western Blots of the Parental and Resistant Cell Lines

Western blot analysis was used to measure basal signalling in the resistant cell lines versus the parental cell line (Figure 3.11. and Figure 3.12.). Phosphorylated CHK1 (S296) was not detected in the parental or either of the resistant cell lines. One possible explanation for this is that levels of phosphorylated CHK1 are so low that they are beyond the limits of antibody detection. In addition, the total amount of CHK1 remained unchanged in the resistant cell lines when compared to the parental cell line.

The levels of phosphorylated CHK2 (S516) in the SRA737- and Prexasertib-resistant cell lines were relatively consistent with those in the parental cell line. The autophosphorylation of CHK2 on residue S516 is required for CHK2 activation (Wu and Chen, 2003). Replication stress can lead to the activation of ATM following DSB formation (Zeman and Cimprich, 2014), which in turn results in the phosphorylation of CHK2 triggering its subsequent activation (Cai, Chehab and Pavletich, 2009). Therefore, the levels of phosphorylated CHK2 in the resistant cell lines versus the parental cell line may indicate that the basal level of replication stress is unchanged in the resistant cell lines with respect to the parental cell line.

The levels of Cyclin A, E, D and B were all increased in the SRA737- and Prexasertib-resistant cell lines with respect to the parental cell line. The Cyclins are each associated with a particular phase of the cell cycle. For example, Cyclin B becomes active during the G2 phase of the cell cycle and is required for entry into mitosis (Hochegger, Takeda and Hunt, 2008). Therefore, the Cyclin levels may indicate that the resistant cell lines are spending longer in each phase of the cell cycle.

4.3.6 Dose-Response of Parental and Resistant Cell Lines to Prexasertib

Western blot analysis was used to investigate changes in DDR signalling in the parental versus the Prexasertib-resistant cell line in response to increasing concentrations of Prexasertib (Figure 3.13.). Prexasertib induced the phosphorylation of CHK1 on S345 in both the parental and the Prexasertib-resistant cell line. The levels of phosphorylated CHK1 remained relatively consistent in both the parental and Prexasertib-resistant cell lines in response to increasing concentrations of Prexasertib, however lower levels of phosphorylated CHK1 were found in the Prexasertib-resistant cell line when compared to the parental cell line. It has been shown that CHK1 inhibition results in the activation of ATR, in part through Cdc25A stabilisation which in turn results in the activation of CDK2. The activation of CDK2 results in increased loading of replication factor Cdc45 and subsequently increased firing of replication origins. This is accompanied by increased binding of RPA to ssDNA which results in the activation of ATR (Syljuåsen *et al.*, 2005).

The total amount of CHK1 decreased in both the parental and Prexasertib-resistant cell lines in response to increasing concentrations of Prexasertib. ATR phosphorylates CHK1 on residue S345 and in turn promotes the ubiquitin-dependent proteasomal degradation of CHK1 (Zhang *et al.*, 2005). The S345 phosphorylation exposes a degron-like motif at the carboxyl-terminus of CHK1 to an Fbx6-containing SCF (Skp1-Cul1-F box) E3 ligase, which in turn mediates the ubiquitination and proteasomal degradation of CHK1 (Zhang *et al.*, 2009).

The WEE1 kinase levels decreased in the parental cell line but remained unchanged in the Prexasertib-resistant cell line in response to increasing concentrations of Prexasertib. In addition, the levels of phosphorylated CDK1 (Y15) decreased in the Prexasertib-resistant cell line but remained relatively consistent in the parental cell line in response to increasing concentrations of Prexasertib. Normally, CHK1 phosphorylates and activates the WEE1 kinase, which subsequently inhibits CDK1 by phosphorylation on inhibitory residue Y15 (O'Connell *et al.*, 1997).

There was strong induction of γH2AX and p21 in the parental cell line in the presence of increasing concentrations of Prexasertib, but very limited induction in the Prexasertib-resistant cell line. One explanation for this is that the Prexasertib-resistant cell line is faster or more proficient at DNA repair than the parental cell line. Otherwise, one might expect to see a stronger induction of γH2AX in the Prexasertib-resistant cell line as it is a marker of DSB formation (Podhorecka, Skladanowski and Bozko, 2010). The protein p21 is a cyclin-dependent kinase inhibitor that promotes cell cycle arrest and provides time for DNA repair (Abbas and Dutta, 2009). Therefore, if the Prexasertib-resistant cell line was faster or more proficient at repairing its DNA then one would expect to see limited induction of p21.

Future Work

To investigate whether the Prexasertib-resistant cell line is faster than the parental cell line at repairing damaged DNA, one might assess the DNA repair dynamics of the cells by measuring the formation of γH2AX foci where γH2AX is a marker of DNA damage. The formation of γH2AX foci can be measured by immunofluorescence using specific γH2AX antibodies to demonstrate its location in chromatin foci at the site of DNA damage (Kuo and Yang, 2008). If the Prexasertib-resistant cell line was faster than the parental cell line at repairing damaged DNA, one might expect to see the disappearance of γH2AX foci in the Prexasertib-resistant cell line before the parental cell line.

Prexasertib resistance was investigated using a candidate approach, focusing on specific targets from the DDR pathway that are known to play a role in the development of chemotherapeutic resistance. Contrastingly, SRA737 resistance may be investigated using an unbiased approach such as genome-wide analysis, which can be used to identify mRNAs that are differentially expressed in the SRA737-resistant cell line versus the parental cell line. The importance of those mRNAs in the development of SRA737 resistance may then be validated and further investigated using small molecule inhibitors and siRNAs where available.

Conclusion

In conclusion, we have generated two resistant cell lines from the PEO1 ovarian cancer cell line: one resistant to SRA737 and the other resistant to Prexasertib. The SRA737- and Prexasertib-resistant cell lines were not only resistant to their respective CHK1 inhibitor but were cross-resistant to Prexasertib and SRA737 respectively. The resistant cell lines also showed cross-resistance to ATR inhibitor AZD6738 and showed limited sensitivity to ATM inhibitor AZD0156. Western blot analysis of basal DDR proteins revealed some changes in DDR signalling between the parental versus the resistant cell lines. However, the most significant findings came from the dose-response western blots, in which we saw strong induction of γH2AX in the parental cell line in response to increasing concentrations of Prexasertib, but very limited induction in the Prexasertib-resistant cell line, which may suggest that DNA repair plays a critical role in the development of Prexasertib resistance. Given that SRA737 and Prexasertib are both ATP-competitive inhibitors of CHK1 they may have similar mechanisms of resistance, however this hypothesis would require further investigation.

References

Abbas, T. and Dutta, A. (2009) 'p21 in cancer: intricate networks and multiple activities', *Nature Reviews Cancer*. Nature Publishing Group, 9(6), pp. 400–414. doi: 10.1038/nrc2657.

Alqahtani, F. Y. *et al.* (2019) 'Paclitaxel', *Profiles of Drug Substances, Excipients and Related Methodology*. Academic Press, 44, pp. 205–238. doi: 10.1016/BS.PODRM.2018.11.001.

Awasthi, P., Foiani, M. and Kumar, A. (2015) 'ATM and ATR signaling at a glance', *Journal of Cell Science*, 128(23), pp. 4255–4262. doi: 10.1242/jcs.169730.

Berek, J. S., Crum, C. and Friedlander, M. (2015) 'Cancer of the ovary, fallopian tube, and peritoneum', *International Journal of Gynecology & Obstetrics*. John Wiley & Sons, Ltd, 131, pp. S111–S122. doi: 10.1016/j.ijgo.2015.06.007.

Boyd, L. R. and Muggia, F. M. (2018) 'Carboplatin/Paclitaxel Induction in Ovarian Cancer: The Finer Points.', *Oncology (Williston Park, N.Y.)*, 32(8), pp. 418–20, 422–4. Available at: http://www.ncbi.nlm.nih.gov/pubmed/30153322 (Accessed: 13 August 2019).

Brett M., R. *et al.* (2017) 'Epidemiology of ovarian cancer: a review', *Cancer Biology & Medicine*, 14(1), pp. 9–32. doi: 10.20892/j.issn.2095-3941.2016.0084.

Cai, Z., Chehab, N. H. and Pavletich, N. P. (2009) 'Structure and Activation Mechanism of the CHK2 DNA Damage Checkpoint Kinase', *Molecular Cell*, 35(6), pp. 818–829. doi: 10.1016/j.molcel.2009.09.007.

Dalal, S. N. *et al.* (1999) 'Cytoplasmic localization of human cdc25C during interphase requires an intact 14-3-3 binding site.', *Molecular and cellular biology*, 19(6), pp. 4465–79. doi: 10.1128/mcb.19.6.4465.

Duan, Z., Brakora, K. A. and Seiden, M. V (2004) 'Inhibition of ABCB1 (MDR1) and ABCB4 (MDR3) expression by small interfering RNA and reversal of paclitaxel resistance in human ovarian cancer cells.', *Molecular cancer therapeutics*, 3(7), pp. 833–8. Available at: http://www.ncbi.nlm.nih.gov/pubmed/15252144 (Accessed: 28 July 2019).

Dumaz, N. and Meek, D. W. (1999) 'Serine15 phosphorylation stimulates p53 transactivation but does not directly influence interaction with HDM2.', *The EMBO Journal*. European Molecular Biology Organization, 18(24), p. 7002. doi: 10.1093/EMBOJ/18.24.7002.

Emery, C. M. *et al.* (2009) 'MEK1 mutations confer resistance to MEK and B-RAF inhibition', *Proceedings of the National Academy of Sciences*, 106(48), pp. 20411–20416. doi: 10.1073/pnas.0905833106.

Falck, J. *et al.* (2001) 'The ATM–Chk2–Cdc25A checkpoint pathway guards against radioresistant DNA synthesis', *Nature*. Nature Publishing Group, 410(6830), pp. 842–847. doi: 10.1038/35071124.

Fletcher, J. I. *et al.* (2010) 'ABC transporters in cancer: more than just drug efflux pumps', *Nature Reviews Cancer*, 10(2), pp. 147–156. doi: 10.1038/nrc2789.

Garrett, M. D. and Collins, I. (2011) 'Anticancer therapy with checkpoint inhibitors: what, where and when?', *Trends in Pharmacological Sciences*, 32(5), pp. 308–316. doi: 10.1016/j.tips.2011.02.014.

Go, R. S. and Adjei, A. A. (1999) 'Review of the Comparative Pharmacology and Clinical Activity of Cisplatin and Carboplatin', *Journal of Clinical Oncology*, 17(1), pp. 409–409. doi: 10.1200/JCO.1999.17.1.409.

Han, L. Y. and Coleman, R. L. (2007) 'Ovarian Cancer Staging', *Operative Techniques in General Surgery*. W.B. Saunders, 9(2), pp. 53–60. doi: 10.1053/J.OPTECHGENSURG.2007.08.002.

Han, X. *et al.* (2016) 'Conformational Change of Human Checkpoint Kinase 1 (Chk1) Induced by DNA Damage.', *The Journal of biological chemistry*. American Society for Biochemistry and Molecular Biology, 291(25), pp. 12951–9. doi: 10.1074/jbc.M115.713248.

Harris, S. L. and Levine, A. J. (2005) 'The p53 pathway: positive and negative feedback loops', *Oncogene*, 24(17), pp. 2899–2908. doi: 10.1038/sj.onc.1208615.

Hata, A. N. *et al.* (2016) 'Tumor cells can follow distinct evolutionary paths to become resistant to epidermal growth factor receptor inhibition', *Nature Medicine*. Nature Publishing Group, 22(3), pp. 262–269. doi: 10.1038/nm.4040.

Hochegger, H., Takeda, S. and Hunt, T. (2008) 'Cyclin-dependent kinases and cell-cycle transitions: does one fit all?', *Nature Reviews Molecular Cell Biology*, 9(11), pp. 910–916. doi: 10.1038/nrm2510.

Hongo, A. *et al.* (1994) 'A comparison of in vitro platinum-DNA adduct formation between carboplatin and cisplatin.', *The International journal of biochemistry*, 26(8), pp. 1009–16. Available at: http://www.ncbi.nlm.nih.gov/pubmed/8088411 (Accessed: 16 August 2019).

Huen, M. S. and Chen, J. (2008) 'The DNA damage response pathways: at the crossroad of protein modifications', *Cell Research*, 18(1), pp. 8–16. doi: 10.1038/cr.2007.109.

Hughes, B. T. *et al.* (2013) 'Essential role for Cdk2 inhibitory phosphorylation during replication stress revealed by a human Cdk2 knockin mutation', *Proceedings of the National Academy of Sciences of the United States of America*. National Academy of Sciences, 110(22), p. 8954. doi: 10.1073/PNAS.1302927110.

Hutchinson, L. (2010) 'PARP inhibitor olaparib is safe and effective in patients with BRCA1 and BRCA2 mutations', *Nature Reviews Clinical Oncology*, 7(10), pp. 549–549. doi: 10.1038/nrclinonc.2010.143.

Johannessen, C. M. *et al.* (2013) 'A melanocyte lineage program confers resistance to MAP kinase pathway inhibition', *Nature*, 504(7478), pp. 138–142. doi: 10.1038/nature12688.

de Jong, M. C. *et al.* (2001) 'Peptide transport by the multidrug resistance protein MRP1.', *Cancer research*, 61(6), pp. 2552–7. Available at: http://www.ncbi.nlm.nih.gov/pubmed/11289130 (Accessed: 28 July 2019).

King, C. *et al.* (2015) 'LY2606368 Causes Replication Catastrophe and Antitumor Effects through CHK1-Dependent Mechanisms', *Molecular Cancer Therapeutics*. American Association for Cancer Research, 14(9), pp. 2004–2013. doi: 10.1158/1535-7163.MCT-14-1037.

Kobayashi, S. *et al.* (2005) '*EGFR* Mutation and Resistance of Non–Small-Cell Lung Cancer to Gefitinib', *New England Journal of Medicine*. Massachusetts Medical Society , 352(8), pp. 786–792. doi: 10.1056/NEJMoa044238.

Kuo, L. J. and Yang, L.-X. (no date) 'Gamma-H2AX - a novel biomarker for DNA double-strand breaks.', *In vivo (Athens, Greece)*, 22(3), pp. 305–9. Available at: http://www.ncbi.nlm.nih.gov/pubmed/18610740 (Accessed: 15 August 2019).

Ledermann, J. *et al.* (2012) 'Olaparib Maintenance Therapy in Platinum-Sensitive Relapsed Ovarian Cancer', *New England Journal of Medicine*. Massachusetts Medical Society , 366(15), pp. 1382–1392. doi: 10.1056/NEJMoa1105535.

Lee, J.-M. *et al.* (2018) 'Prexasertib, a cell cycle checkpoint kinase 1 and 2 inhibitor, in BRCA wild-type recurrent high-grade serous ovarian cancer: a first-in-class proof-of-concept phase 2 study', *The Lancet Oncology*, 19(2), pp. 207–215. doi: 10.1016/S1470-2045(18)30009-3.

Lippert, T., Ruoff, H.-J. and Volm, M. (2011) 'Intrinsic and Acquired Drug Resistance in Malignant Tumors', *Arzneimittelforschung*, 58(06), pp. 261–264. doi: 10.1055/s-0031-1296504.

Ludwik, K. A. *et al.* (2016) 'Development of a RSK Inhibitor as a Novel Therapy for Triple-Negative Breast Cancer', *Molecular Cancer Therapeutics*. American Association for Cancer Research, 15(11), pp. 2598–2608. doi: 10.1158/1535-7163.MCT-16-0106.

Masoumi-Moghaddam, S. *et al.* (2015) 'Sprouty2 protein in prediction of post-treatment ascites in epithelial ovarian cancer treated with adjuvant carbotaxol chemotherapy.', *American journal of cancer research*, 5(8), pp. 2498–507. Available at: http://www.ncbi.nlm.nih.gov/pubmed/26396926 (Accessed: 13 August 2019).

Maya, R. *et al.* (2001) 'ATM-dependent phosphorylation of Mdm2 on serine 395: role in p53 activation by DNA damage.', *Genes & development*. Cold Spring Harbor Laboratory Press, 15(9), pp. 1067–77. doi: 10.1101/gad.886901.

McWhinney, S. R., Goldberg, R. M. and McLeod, H. L. (2009) 'Platinum neurotoxicity pharmacogenetics.', *Molecular cancer therapeutics*. NIH Public Access, 8(1), pp. 10–6. doi: 10.1158/1535-7163.MCT-08-0840.

Moll, U. M. and Petrenko, O. (2003) 'The MDM2-p53 interaction.', *Molecular cancer research : MCR*. American Association for Cancer Research, 1(14), pp. 1001–8. Available at: http://www.ncbi.nlm.nih.gov/pubmed/14707283 (Accessed: 13 August 2019).

Nazarian, R. *et al.* (2010) 'Melanomas acquire resistance to B-RAF(V600E) inhibition by RTK or N-RAS upregulation', *Nature*, 468(7326), pp. 973–977. doi: 10.1038/nature09626.

O'Connell, M. J. *et al.* (1997) 'Chk1 is a wee1 kinase in the G2 DNA damage checkpoint inhibiting cdc2 by Y15 phosphorylation', *The EMBO Journal*, 16(3), pp. 545–554. doi: 10.1093/emboj/16.3.545.

Ovarian cancer statistics | Cancer Research UK (no date). Available at: https://www.cancerresearchuk.org/health-professional/cancer-statistics/statistics-by-cancer-type/ovarian-cancer (Accessed: 14 March 2019).

PDQ Adult Treatment Editorial Board, P. A. T. E. (2002) *Ovarian Epithelial, Fallopian Tube, and Primary Peritoneal Cancer Treatment (PDQ®): Patient Version*, *PDQ Cancer Information Summaries*. National Cancer Institute (US). Available at: http://www.ncbi.nlm.nih.gov/pubmed/26389163 (Accessed: 15 August 2019).

Peng, C. *et al.* (1997) 'Mitotic and G2 Checkpoint Control: Regulation of 14-3-3 Protein Binding by Phosphorylation of Cdc25C on Serine-216', *Science*, 277(5331), pp. 1501–1505. doi: 10.1126/science.277.5331.1501.

Podhorecka, M., Skladanowski, A. and Bozko, P. (2010) 'H2AX Phosphorylation: Its Role in DNA Damage Response and Cancer Therapy', *Journal of Nucleic Acids*, 2010, pp. 1–9. doi: 10.4061/2010/920161.

Prat, J. and FIGO Committee on Gynecologic Oncology, F. C. on G. (2015) 'FIGO's staging classification for cancer of the ovary, fallopian tube, and peritoneum: abridged republication.', *Journal of gynecologic oncology*. Korean Society of Gynecologic Oncology and Colposcopy, 26(2), pp. 87–9. doi: 10.3802/jgo.2015.26.2.87.

Roett, M. A. and Evans, P. (2009) 'Ovarian cancer: an overview.', *American family physician*, 80(6), pp. 609–16. Available at: http://www.ncbi.nlm.nih.gov/pubmed/19817326 (Accessed: 13 August 2019).

Shi, H. *et al.* (2012) 'Melanoma whole-exome sequencing identifies V600EB-RAF amplification-mediated acquired B-RAF inhibitor resistance', *Nature Communications*, 3(1), p. 724. doi: 10.1038/ncomms1727.

Shieh, S. Y. *et al.* (2000) 'The human homologs of checkpoint kinases Chk1 and Cds1 (Chk2) phosphorylate p53 at multiple DNA damage-inducible sites.', *Genes & development*. Cold Spring

Harbor Laboratory Press, 14(3), pp. 289–300. Available at: http://www.ncbi.nlm.nih.gov/pubmed/10673501 (Accessed: 13 August 2019).

Sørensen, C. S. *et al.* (2003) 'Chk1 regulates the S phase checkpoint by coupling the physiological turnover and ionizing radiation-induced accelerated proteolysis of Cdc25A', *Cancer Cell*. Cell Press, 3(3), pp. 247–258. doi: 10.1016/S1535-6108(03)00048-5.

Sørensen, C. S. *et al.* (2005) 'The cell-cycle checkpoint kinase Chk1 is required for mammalian homologous recombination repair', *Nature Cell Biology*, 7(2), pp. 195–201. doi: 10.1038/ncb1212.

Syljuåsen, R. G. *et al.* (2005) 'Inhibition of human Chk1 causes increased initiation of DNA replication, phosphorylation of ATR targets, and DNA breakage.', *Molecular and cellular biology*. American Society for Microbiology (ASM), 25(9), pp. 3553–62. doi: 10.1128/MCB.25.9.3553-3562.2005.

Walker, M. *et al.* (2009) 'Chk1 C-terminal regulatory phosphorylation mediates checkpoint activation by de-repression of Chk1 catalytic activity.', *Oncogene*. Europe PMC Funders, 28(24), pp. 2314–23. doi: 10.1038/onc.2009.102.

Walton, M. I. *et al.* (2016) 'The clinical development candidate CCT245737 is an orally active CHK1 inhibitor with preclinical activity in RAS mutant NSCLC and Eµ-MYC driven B-cell lymphoma', *Oncotarget*, 7(3), pp. 2329–42. doi: 10.18632/oncotarget.4919.

Wu, X. and Chen, J. (2003) 'Autophosphorylation of checkpoint kinase 2 at serine 516 is required for radiation-induced apoptosis.', *The Journal of biological chemistry*. American Society for Biochemistry and Molecular Biology, 278(38), pp. 36163–8. doi: 10.1074/jbc.M303795200.

Yap, T. A., Carden, C. P. and Kaye, S. B. (2009) 'Beyond chemotherapy: targeted therapies in ovarian cancer', *Nature Reviews Cancer*, 9(3), pp. 167–181. doi: 10.1038/nrc2583.

Zeman, M. K. and Cimprich, K. A. (2014) 'Causes and consequences of replication stress.', *Nature cell biology*. NIH Public Access, 16(1), pp. 2–9. doi: 10.1038/ncb2897.

Zhang, Y.-W. *et al.* (2005) 'Genotoxic Stress Targets Human Chk1 for Degradation by the Ubiquitin-Proteasome Pathway', *Molecular Cell*, 19(5), pp. 607–618. doi: 10.1016/j.molcel.2005.07.019.

Zhang, Y.-W. *et al.* (2009) 'The F Box Protein Fbx6 Regulates Chk1 Stability and Cellular Sensitivity to Replication Stress', *Molecular Cell*, 35(4), pp. 442–453. doi: 10.1016/j.molcel.2009.06.030.